Spring 5-12-2022

Analyzing the interactions of thermoresponsive coacervate-forming biodegradable polyester encapsulation on model protein structure and activity

Conner Casterline

Analyzing the interactions of thermoresponsive coacervate-forming biodegradable polyester encapsulation on model protein structure and activity

By

Conner Forest Casterline

B.S. Biochemistry

Kennesaw State University, 2020

Thomas C. Leeper Laboratory

Submitted in partial fulfillment of the requirements

For the Degree of Master of Science in Chemical Sciences in the Department of

Chemistry and Biochemistry at Kennesaw State University

May 2022

_____	_____
Committee Chair	Graduate Program Coordinator
_____	_____
Committee Member	Department Chair
_____	_____
Committee Member	College Dean

DEDICATION

To my wonderful family for endlessly supporting me throughout this master's program and helping me along my journey.

ACKNOWLEDGEMENTS

I would like to thank my invaluable research supervisor, Dr. Thomas C. Leeper, for his continuous support and scientific guidance throughout this program. His mentorship has helped transform me into the scientist I am today. I would also like to express my gratitude for my committee members, Dr. Carol A. Chrestensen and Dr. Christopher R. Dockery, for their critical feedback pertaining to my research and writing. I would like to thank my collaborator, Dr. Abraham Joy and his laboratory at the University of Akron, for providing the valuable resources to pursue my research. Lastly, I would like to thank Kennesaw State University and the Department of Chemistry and Biochemistry for the opportunity to learn and to gain experience within this program.

ABSTRACT

Protein therapeutics hold high efficacy in treatment for various diseases including cancer and diabetes. However, the treatment cost is generally higher than other therapeutics mainly due to *in vivo* protein degradation. This drawback creates demand for more efficient delivery methods to preserve the function and integrity of protein therapeutics. Thermoresponsive coacervate-forming biodegradable polyesters (TR-PEs) are a thermoresponsive molecular packaging system used in protein therapeutic research. The term coacervate refers to a phase-separated solution in which a dense polymer phase separates from the aqueous phase to form nanodroplets within solution, capturing bioactive molecules. Limited research demonstrates if TR-PEs can encapsulate and preserve a larger protein's activity and how these TR-PEs interact with a protein on the biophysical level. It was determined that TR-PEs encapsulated and released active β-galactosidase enzyme. Encapsulation was visualized using confocal fluorescence microscopy and by labeling β-galactosidase with fluorescein isothiocyanate. Interactions between ^{15}N-isotopically labelled human ubiquitin c and TR-PEs were investigated through variable temperature nuclear magnetic resonance. It was interpreted that TR-PEs non-specifically interact with ^{15}N-ubiquitin and that various pendant groups within a given polymer resulted in non-significant differences. Although TR-PEs may not be specifically interacting with the model cargos, demonstrating that TR-PEs capture and release an unaltered, complex protein exemplifies the viability of using TR-PEs for future therapeutic packaging and possible delivery.

TABLE OF CONTENTS

TABLE OF CONTENTS

LIST OF TABLES

LIST OF FIGURES

LIST OF ABBREVIATIONS

ADME	Absorption, distribution, metabolism, and excretion
β-gal	β-galactosidase
BSA	Bovine serum albumin
CEC	Cation exchange chromatography
CFM	Confocal fluorescence microscopy
CPR	Chlorophenol red
CPRG	Chlorophenol red galactopyranoside
CSB	Chemical shift broadening
CSP	Chemical shift perturbation
CSS	Chemical shift sharpening
E. coli	*Escherichia Coli*
EDTA	Ethylenediaminetetraacetic acid
FITC	Fluorescein isothiocyanate
HSQC	Heteronuclear single quantum coherence
IEC	Ion exchange chromatography

IMAC	Immobilized metal affinity chromatography
IPTG	Isopropyl β-d-1-thiogalactopyranoside
LB	Lysogeny broth
LCST	Lower Critical solution temperature
LOD	Limit of Detection
NMR	Nuclear magnetic resonance
RT	Room temperature
SEC	Size exclusion chromatography
STD	Saturation transfer difference
TR-PEs	Thermoresponsive polyesters
VT	Variable temperature

Chapter One

BACKGROUND AND SIGNIFICANCE

Modern medicine must adapt to the demand for more effective therapeutics. As medicine moves toward using biomacromolecules, i.e., mRNA vaccines, antibodies, and proteins, the stabilization and controlled release of these delicate molecules will become an important concern. Every therapeutic intrinsically contains pharmacokinetic characteristics including absorption, distribution, metabolism, and excretion (ADME). Drug optimization includes improving one or more pharmacokinetic aspects. For example, if researchers hypothesize that a drug will have a higher efficacy if its half-life is increased, then they might target the metabolism of the drug and attempt to decrease the rate of metabolism from the body by protecting the therapeutic with a delivery system.[1] The work described herein, concerns optimization and analysis of a novel nanoparticle scale protein delivery system with the capacity to tune pharmacokinetics. The following chapter provides a brief historical context for this system.

A large portion of the drug market is occupied by protein therapeutics.[2] Protein therapeutics were originally extracted and purified from natural sources, such as insulin. While revolutionizing medicine in the 1920's, the steep cost for purified protein limited its benefits. Current protein therapeutics are still derived from naturally occurring proteins but are now typically modified to optimize both biological response and production. Recombinant protein production was introduced in 1979 when synthetic

human insulin was cloned into *Escherichia Coli (E. coli)*.[3] This innovation decreased the cost of insulin production while retaining efficacy as a treatment method. When compared to mammalian expression, the recombinant proteins hold similarly processed proteins and have increase half-life and *in vivo* potency.[4]

Although protein drugs are critical for treating diseases like diabetes and cancer, these therapeutics typically have a complex manufacturing process that is magnitudes more expensive than small-molecule drug synthesis. Relative to small-molecule drugs, there is increased regulation and requirements for the protein drug manufacturing process to ensure a biologically sound product is purified.[5] Thus, the production is typically more expensive and time consuming. Other challenges facing protein therapeutics are premature degradation and immunogenicity, an induced immune response.[6] Premature degradation can often lead to a lack of distribution, from increased drug metabolism, as well as premature excretion. In turn, the dosage of the medicine must be increased greatly to obtain a desirable biological response. When looking to optimize protein molecules that have therapeutic potential, delivery systems have the possibility of increasing distribution by decreasing metabolism and excretion, and possibly decreasing toxicity as well.

There are various drug delivery methods available, however, an emerging class of delivery systems are a polyester-based protein encapsulation. Nanogels consist of covalently crosslinked polymer networks. The polymer networks are designed to take on a shell and core architecture. The shell is typically zwitterionic to increase the nanogel's stability and solubility. The nanogel core can be modified to respond to external stimuli, like pH or temperature.[7] This response allows the core to swell and attract biomolecules

in this hydrophilic state. The attraction is encouraged by tuning the core to contain positive charge, which attracts negatively charged proteins. Certain nanogels can be effectively degraded in acidic pH, which results in the downstream metabolism of polymer units. Nanogels are theorized to be effective in medical imaging where contrast agents are encapsulated and then are administered to improve imaging effectiveness.[8] The FDA has yet to approve nanogels for medicinal trials citing toxicity issues due to degradation products. This opens the door for an alternate therapeutic packaging system with fewer cytotoxic metabolites.

Coacervate-forming biodegradable thermoresponsive polyesters (TR-PEs) are another polymer encapsulation system. The most important characteristic of these TR-PEs is the ability to spontaneously change phases from hydrophilic to hydrophobic when rising above a lower critical solution temperature (LCST).[9] Similarities between the coacervates and nanogels include thermoresponsive characteristics and acidic degradation. Unlike nanogels, TR-PEs are shown to have relatively low cytotoxicity, which minimizes future concern for downstream metabolites within the human body. The most critical difference between nanogels and TR-PEs is the structural formation. Instead of the covalently crosslinked polymer networks found in nanogels, TR-PEs are monomeric in solution. When the temperature is increased above the LCST, the monomeric units spontaneously self-assemble into coacervate droplets that can encapsulate biomolecules. In addition, this process is reversible. Upon cooling to below the LCST, the coacervates dissipate into the aqueous phase and any captured biomolecules would be released. The polymer units also have tunable pendant groups that increase affinity for a target molecule[10]. Furthering the development of efficient and

protective delivery methods for therapeutics could allow lower therapeutic dosages to illicit the same efficacy as previous treatment methods. This would revolutionize protein therapeutic treatments by decreasing cost of lifesaving medicine, making them more affordable and accessible to all communities.

The encapsulation of model proteins is used to demonstrate the effectiveness and viability of using various TR-PEs for therapeutic delivery. Model proteins are easily produced and purified and can have a wide range of characteristics. Insulin, bovine serum albumin (BSA), β-galactosidase (β-gal), and ubiquitin are examples of model proteins. TR-PEs are most efficient at capturing smaller proteins like insulin and BSA that are between 6 kDa and 66.5 kDa respectively. Previous nanogel research demonstrates β-gal was encapsulated with a 35% efficiency[9]. β-gal is a large homotetramer (~460 kDa). It is a hydrolase that catalyzes the hydrolysis of the β-1-4 galactosidic bond of lactose. The large molecular weight of β-gal stretches the limit of nanogel encapsulation ability due to a minimum requirement of crosslinked polymers within the nanogel to preserve overall stability. Furthermore, studies previously testing the encapsulation efficiency of coacervate-forming TR-PEs included testing with insulin and BSA but did not include β-gal for analysis[10]. Testing the effects of encapsulation on β-gal activity using the coacervate-forming TR-PEs has the possibility of establishing a more efficient method of capturing larger therapeutic biomolecules.

Investigating the biophysical model protein-polymer interactions, at an individual amino acid resolution, required human ubiquitin c. This model protein is a small, thermostable, monomeric protein (~8.6 kDa). It has optimal characteristics for use in nuclear magnetic resonance biophysical studies. This enabled examination of various TR-

PEs and how these molecules interacted while TR-PEs were within both the aqueous and coacervate phases. This provided insight on if TR-PEs, with varying pendent groups, specifically interacted with surface amino acids to encourage encapsulation.

Three goals of this project were investigated and follow:

1. Developed and optimized expression and purification protocols for individual model cargo proteins using immobilized metal affinity chromatography and ion exchange chromatography purification methods.
2. Determined the effects of TR-PE interactions on a model protein's specific activity and structure with colorimetric assay assessments and nuclear magnetic resonance analysis.
3. Evaluated the encapsulation efficiency of model cargo proteins incorporating fluorometric and colorimetric assays.

Protocols for model protein expression and purification were developed and optimized to produce pure and sufficient protein yields for analysis. A former graduate student in the Leeper laboratory, Aaron Schultz, outlined a protein purification protocol for a protein commonly expressed in the lab, *Pseudomonas aeruginosa* Inhibitor Vertebrate Lysozyme, unrelated to this project. This protocol was initially followed to determine baselines for the model protein expression and purifications. There were multiple alterations, explained within subsequent chapters, to accommodate the nuances within expression and purification requirements for each protein.

The specific activity of purified β-gal was determined through colorimetric-based kinetic experiments. Samples within a given encapsulation and release procedure were compared to examine the effects of TR-PE encapsulation on the integrity of β-gal.

Biophysical analysis of ^{15}N-ubiquitin demonstrated the effects of TR-PEs on the protein's structural integrity and that pendant groups, within the copolymer, did not specifically encourage protein-polymer association upon encapsulation.

The encapsulation efficiency of various TR-PEs on β-gal was examined through both colorimetric and fluorometric assays. These provided protein retention rates and evidenced that FITC-β-gal was encapsulated within all tested polymer variants.

These techniques allowed conclusions concerning the effects of coacervate-forming biodegradable thermoresponsive polyester encapsulation on model protein cargos and the potential for future use as a protein packaging system.

Chapter Two

EXPRESSION AND PURIFICATION OF MODEL PROTEINS

Introduction

Biochemistry laboratories frequently use protein expression and purification methods to investigate a specific protein and study its biophysical characteristics or interactions. These methods are crucial for convenient and cost-effective research. Modern protein expression allows customizable design of various protein sequences and purification "tags" to optimize purification yields. One such purification method is immobilized metal affinity chromatography (IMAC). It is designed to isolate proteins with histidine tags using coordinating metals like Ni^{2+} or Co^{2+} within the column. These "His-tags" typically span six to ten consecutive histidine residues at the N or C-terminal end of a protein. IMAC follows a four-step protocol: initial sample loading containing tagged protein, elution and recovery, cleavage of the tag, and second loading to clear the protein from the tags. Upon loading sample to an IMAC column, the His-Tags will interact with the charged metals through coordination chemistry. Interaction strength increases with the count of consecutive histidine within the tag. Proteins may then be eluted from the column by increasing the concentration of imidazole, the functional group of histidine, to displace and replace the protein's histidine interactions. The elution process must be completed with a gradient of increasing imidazole concentration. This is due to the possibility that non-tagged proteins may interact with the column when

histidine residues are adjacent within their tertiary structure. A high imidazole concentration within the sample will present a problem in subsequent purification steps.

Once the fraction with the desired protein is identified, the imidazole concentration must be reduced, any nickel ions from the columns chelated, and the six-histidine tag cleaved from β-gal. As mentioned previously, it is possible for non-tagged proteins to weakly interact with the column via tertiary structure. Sample with high imidazole concentration will prevent those histidine interactions and will allow the His-Tag to also coelute with the desired protein upon the second column loading step. Therefore, imidazole concentration should be reduced with dialysis to prevent those circumstances. It is possible that nickel ions coelute with sample. Disodium ethylenediaminetetraacetic acid (EDTA) should be added to the sample to chelate these nickel ions to prevent any further interaction with the histidine tag present on the sample. Completing the preparation for purification, the histidine tag must be cleaved from β-gal with thrombin protease. Prior to the second loading step, a benzamidine column is placed in line with the nickel column to withhold the thrombin from contaminating the purified β-gal. Size exclusion chromatography (SEC) assists final purification through separation of proteins by molecular weight. SEC is employed to further purify β-gal from any possible contaminants.

Although β-gal and ubiquitin follow the same general expression and purification protocol, the major differences include the use of M9 minimal media and addition of ^{15}N-labelled ammonium chloride.[11] The labelled ammonium chloride is added to the minimal media to encourage bacteria to use ^{15}N upon induction. This will make it more likely that ubiquitin protein will be labeled and can be effectively used in 2D NMR. The

recombinant human ubiquitin does not contain a His-tag, therefore an alternative purification method must be followed.

Ion exchange chromatography (IEC) is a protein purification method that relies on charge differences between various proteins within a sample. Specifically, cation exchange chromatography (CEC) separates proteins that hold negative net charge from proteins with positive net charge. Purifying the recombinant human ubiquitin protein requires CEC followed by SEC to purify the protein. Elution from the CEC column requires a gradient process with buffer ranging from 0.5 M to 1.0 M NaCl. The ionic strength from the chloride ions will displace the charge-charge interaction between protein and charged resin. High salt concentration within sample will interfere with SEC purification. Therefore, ubiquitin's salt concentration must be reduced with dialysis. Although CEC holds less purifying capacity relative to IMAC purification, it is useful when purifying smaller proteins that may not retain structure if a sequenced tag, like a His-Tag, is fused to the protein. Thus, following CEC with SEC will aid the purification of ubiquitin.

Experimental

A protein expression and IMAC purification protocol, followed with SEC clarification, were used to obtain pure β-gal. A patented plasmid (Patent # 11,125,743), pAT_T7_HisLacZ, was sourced from Dr. Alexander Green.[12] This plasmid expresses a modified LacZ gene, producing β-gal with a N-terminal six-histidine tag and a thrombin protease cleavage recognition site. The plasmid is mediated by the isopropyl β-d-1-

thiogalactopyranoside (IPTG) inducible T7 promoter and has ampicillin resistance for selectivity. The plasmid was received and transformed into competent DH5α *E. coli* cells and plated onto lysogeny broth (LB)-agar plates with ampicillin antibiotics. A colony from the transformed DH5α *E. coli* cells was inoculated and incubated overnight in a shaker at 37°C. Following a miniprep with E.Z.N.A.® Plasmid DNA Mini Kit II (*Omega Bio-Tek*), the resulting plasmid concentration was determined to be 151.3ng/μL with a NanoDrop™ One (*Thermo Scientific*). The sequence was validated using *Genewiz* sanger sequencing and the six-histidine tag and thrombin protease cleavage site were identified.

The amplified plasmid was then transformed into competent BL21(DE3) *E. Coli* cells and streaked onto LB-agar plates with ampicillin antibiotic and incubated overnight. Colonies were inoculated into two 50mL sterile LB media solutions with ampicillin and incubated overnight in a shaker at 37°C. The small cultures were transferred to two 1L sterile LB media solutions with ampicillin. The large cultures were incubated at 37°C and induced with 1mM IPTG once the $O.D._{600}$ reached 0.6. They were incubated overnight in a shaker at 22°C. The cultures were centrifuged 12,000 rpm at 4°C for fifteen minutes. The supernatant was discarded, and pellets were resuspended in Buffer A (**Appendix 1.1**). The mixture was homogenized and lysed with a French press. The crude lysate was centrifuged 27,000 rpm at 4°C for forty-five minutes and the supernatant was recovered.

The supernatant was purified with a Bio-Rad™ FPLC NGC Chromatography System with nickel based IMAC and then followed with SEC for clarification. The elution sample was spiked with 0.1% v/v disodium EDTA and dialyzed within Buffer A for approximately 24 hours. Thrombin, 100 uL at 0.5 units/uL, was added for His-tag cleavage and then dialysis was continued to further reduce imidazole concentration. A

HiTrap™ Benzamidine FF (HS) column was installed subsequent to a HisTrap™ FF Crude column and the flowthrough was collected and concentrated. Concentrated sample was loaded for SEC with a HiLoad Superdex SD75 16x600 mm preparative column (*Agilent/GE*). Fractions representing purified β-gal were pooled and concentrated to 4 mL. Samples were obtained throughout expression and purification to assess the purity of the final sample with SDS-PAGE. The gel was stained with Coomassie Brilliant Blue™ for band visualization.

The recombinant human ubiquitin plasmid was originally from Rachel Klevit's laboratory obtained from Addgene (Plasmid #: 12647). This plasmid expresses wild type human ubiquitin C, contains ampicillin resistance, and is regulated by the IPTG inducible T7 promoter. The plasmid was 63 ng/uL for transformation into competent BL21(DE3) *E. coli* cells. M9 minimal media was made, filter sterilized, and then ampicillin antibiotics were added. Small cultures were inoculated into three flasks each with 100 mL of M9 minimal media and incubated in a shaker overnight at 37°C. Upon equal distribution into four flasks with 1.5 L of M9 minimal media, the large cultures were incubated at 37°C. Once the $O.D._{600}$ reached 0.6, 3.0 g of dextrose, 0.75 g of ^{15}N-labeled ammonium chloride (*Cambridge Isotope Labs*), and 1 mM IPTG were added. The cultures were incubated overnight in a shaker at 22°C. Cultures were centrifuged 12,000 rpm at 4°C for fifteen minutes. The supernatant was discarded. Cell pellets were resuspended and homogenized in Buffer C (**Appendix 1.2**). This was followed by French Press lysis and centrifugation at 27,000 rpm at 4°C for forty-five minutes and the clarified lysate was recovered.

The supernatant was purified with a Bio-Rad™ FPLC NGC Chromatography System using CEC and was followed with SEC clarification. Clarified lysate was loaded into a HiPrep™ SP FF 16/10 column for CEC. After absorbance returned to baseline, the sample was eluted with an increasing gradient ranging 0-10-15-25-100% Buffer D at 0.5 %/mL of eluant (**Appendix 1.2**). Samples were collected in 4 mL fractions and were screened for ubiquitin with SDS-PAGE. Ubiquitin containing fractions were pooled and dialyzed in 1x PBS pH 7.4 (**Appendix 1.2**). The sample was concentrated and loaded into a HiLoad Superdex SD75 16x600 mm preparative column (*Agilent/GE*) for SEC. The sample was facilitated through the column with 1x PBS pH 7.4 and collected in fractions of 4 mL. Fractions were again screened for ubiquitin presence with SDS-PAGE. Fractions containing only expected bands for ubiquitin were pooled and concentrated to 3.5 mL. Other samples were collected throughout the expression and purification to analyze quality and purity of the final sample with SDS-PAGE.

Results

Purification of β-gal using an IMAC with the cleave and clear protocol was straightforward. The chromatogram for the first IMAC step shows two main peaks (**Figure 2.1a**). The first peak, volumes 2mL-70mL, shows flowthrough of any biological molecules lacking nickel affinity. The second peak, volumes 84mL-112mL, indicates presence of the his-tagged β-gal in the elution fractions. Due to the possibility that other proteins may have affinity for the column from local histidine residues interacting with nickel ions, the percent of imidazole wash was increased using a gradient of Buffer B (**Appendix 1.1**) to limit sample contamination.

Thrombin protease recognizes a cleavage site inserted between the β-gal sequence and the N-terminal six histidine tag. When thrombin hydrolyzes the linkage, it does not remain bound to the tag. Therefore, it is important to install a HiTrap™ Benzamidine FF (HS) column subsequent to the HisTrap™ FF Crude column to capture thrombin. The cleaved his-tags within the sample were bound to the charged nickel column and thrombin flowed through and bound to the benzamidine column. B-gal flowed through both columns and was initially collected between volumes 2mL and 42mL (**Figure 2.1b**). SEC results demonstrated that β-gal was purified by appearance of a single peak at the expected elution volumes, 40mL-68mL (**Figure 2.1c**).

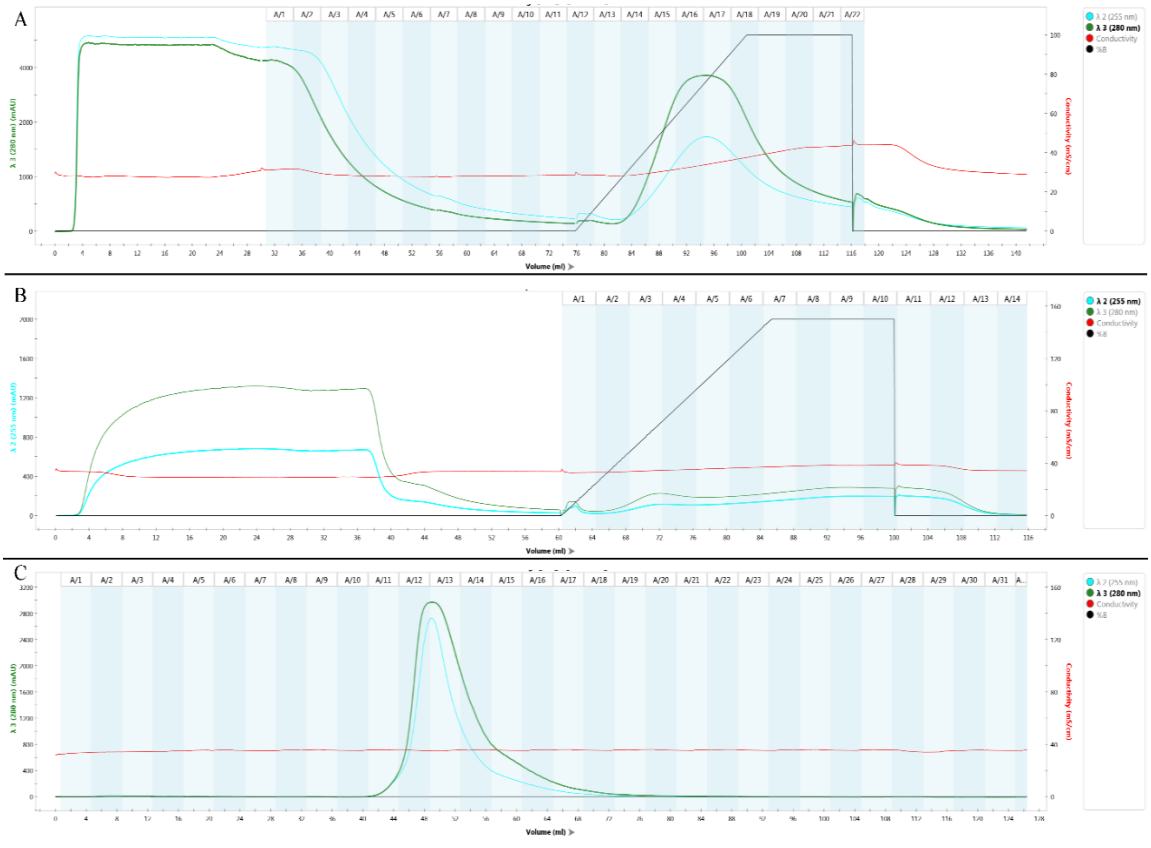

Figure 2.1. (**A**) Chromatogram from the first step of IMAC. His-β-gal appears and was collected between volumes 84mL and 112mL. (**B**) Chromatogram from second IMAC

step. B-gal flows through columns and appears and was collected between volumes 2mL and 42mL. (**C**) Chromatogram from SEC. β-gal appears at the expected volume of 48mL.

The samples collected throughout the expression and purification were electrophoresed on an 12% SDS-PAGE gel to assess sample purity. A band at the expected location of β-gal indicates that pure protein is obtained (**Figure 2.2**). The protocol, with minor changes from a standard expression and purification protocol, is effective at purifying β-gal.

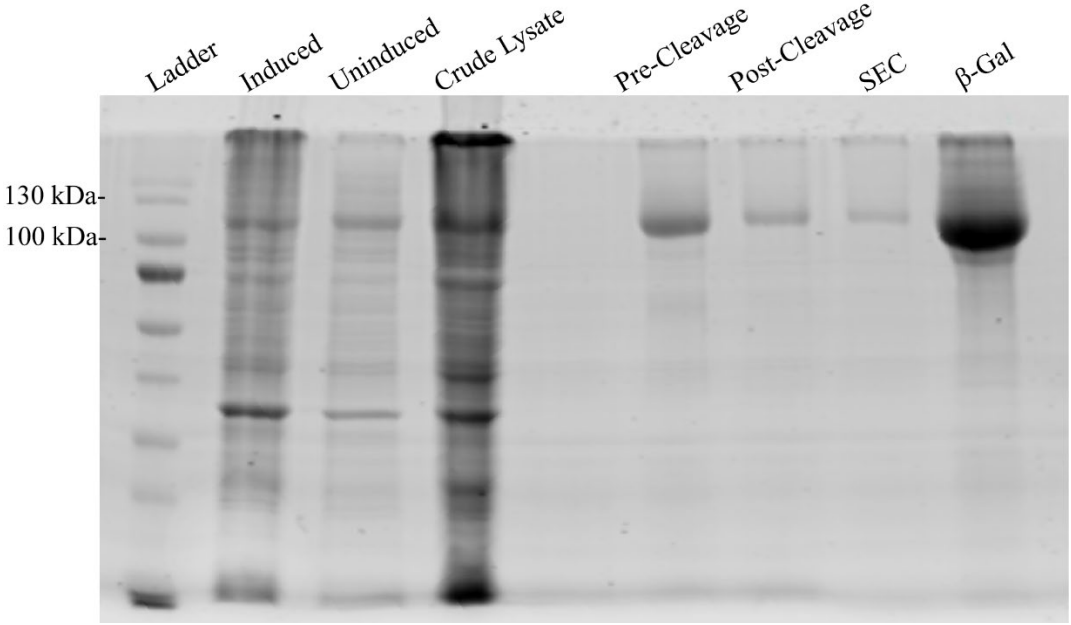

Figure 2.2. SDS-PAGE gel electrophoreses of samples from β-gal expression and purification. B-gal monomer is a 116kDa and appears at its expected molecular weight as indicated by the PageRuler^{TM} Plus Prestained Protein Ladder.

Ubiquitin purification with CEC and SEC required optimization to identify the ideal elution parameters for the small protein. Fraction samples from each purification step were electrophoresed with 20% SDS-PAGE to locate fractions containing ubiquitin

before proceeding. Modifying the elution gradient step for CEC resulted in isolating ubiquitin with impurities. This sample was pooled from fractions A15-A18 (**Figure 2.3A**) and was visualized in lane elution (**Figure 2.4**). Further purification of ubiquitin was conducted with SEC. Ubiquitin appeared with impurities in fractions A18-A20 and was clarified within fractions A21-A25 (**Figure 2.3B**). The final concentrated sample was visualized in the "Post-SEC" lane (**Figure 2.4**). Faint bands are within the final sample appearing around the 25 kDa molecular marker. Their presence was deemed acceptable for purposes of nuclear magnetic resonance experimentation.

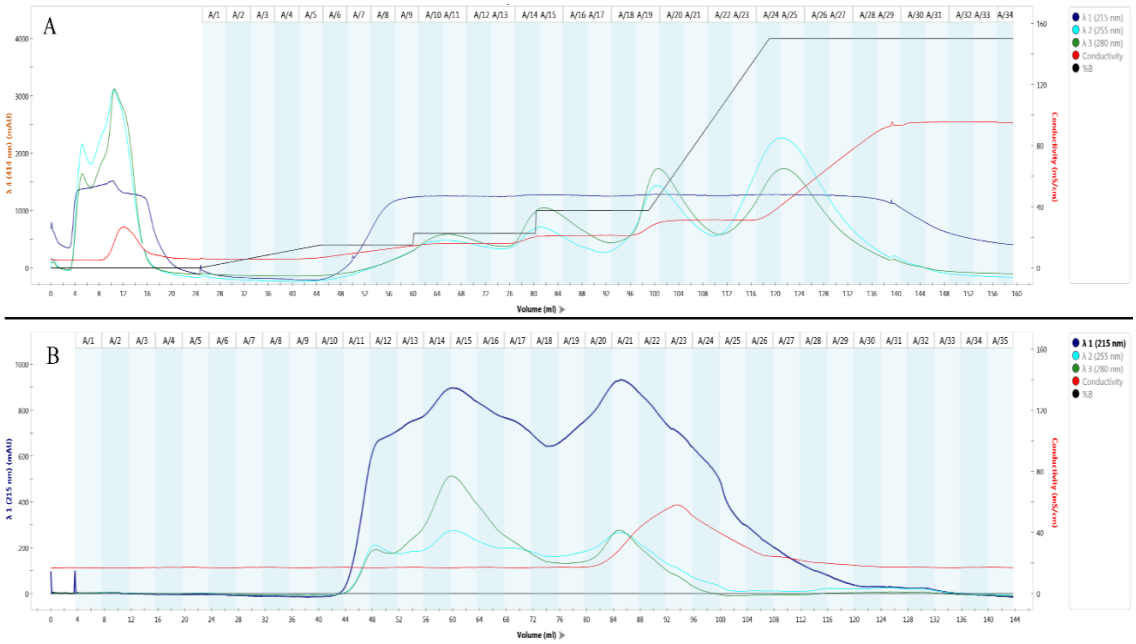

Figure 2.3. (**A**) Chromatogram representing CEC of ubiquitin. SDS-PAGE gel electrophoreses was required to elucidate which fractions contained ubiquitin. (**B**) Chromatogram representing the SEC of ubiquitin. SDS-PAGE gel electrophoreses was conducted to determine the presence of ubiquitin within fractions.

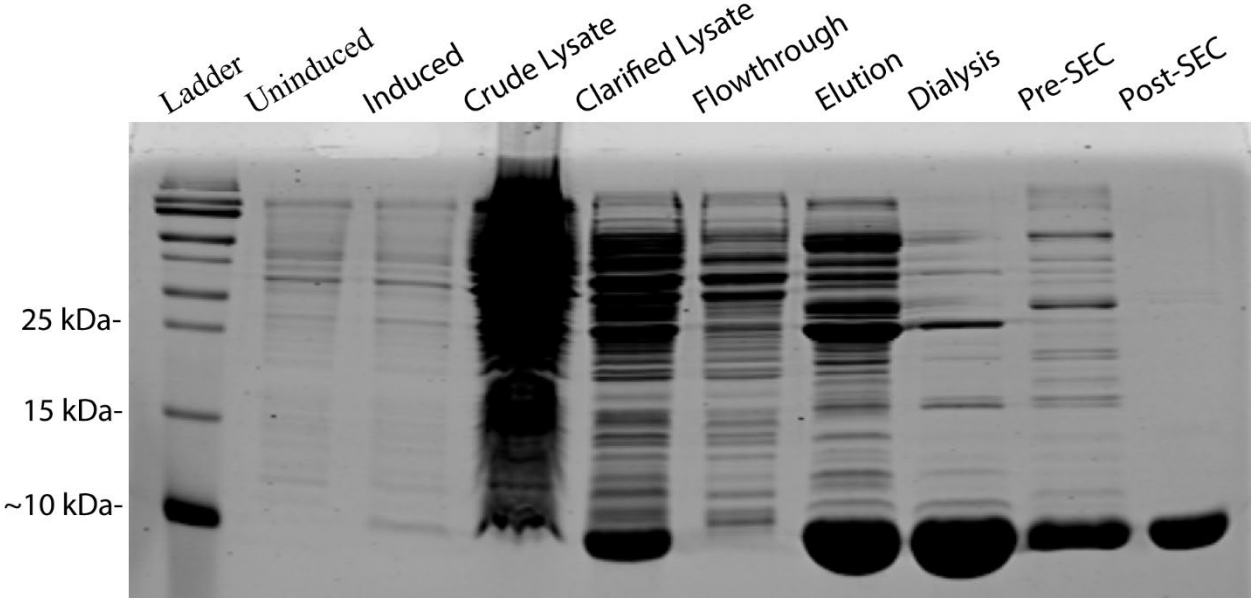

Figure 2.4. 20% SDS-PAGE gel electrophoreses of samples from ubiquitin expression and purification. Ubiquitin is an 8.6 kDa monomer and appears at expected molecular weight as indicated by the PageRuler^{TM} Plus Prestained Protein Ladder.

The expression and purification of both model proteins were optimized for efficiency. There were no direct problems within the β-gal protocol. However, thrombin activity was reduced in the presence of concentrated EDTA or imidazole. Therefore, timing of thrombin addition for cleavage during dialysis after the first IMAC step was most efficient at 24 hours. This time delay allowed sufficient reduction of EDTA and imidazole concentration.

Although ubiquitin expression was straightforward, the purification protocol was initially troublesome and time consuming. The ubiquitin elution volume for CEC was unknown. Every fraction showing increased absorbance was analyzed with SDS-PAGE to determine the presence of ubiquitin. The elution was optimized to an increasing gradient of Buffer D from 0-10-15-25-100%. Ubiquitin was determined to coelute with

impurities around 300 mM NaCl. SEC was employed to further purify the sample. Being 8.6 kDa, ubiquitin was expected to elute off the SEC column in the latter volumes. SDS-PAGE analysis was repeated for all samples showing increased absorbances. It was confirmed that ubiquitin elutes last. Certain fractions contained impurities and were not included in the final sample pool. This resulted in reduced ubiquitin concentration.

Overall, both model proteins provided standard purified yields. B-gal resulted 21.4 mg/L using LB media and the ubiquitin purification yielded 7.56 mg/L using M9 minimal media. Further optimization of purification parameters like fluctuating the reaction time between thrombin and β-gal (resulting in more cleaved product) or modulating the ubiquitin CEC elution gradient (better isolating ubiquitin from coelution) coupled with modifying the flow rate for SEC (ensuring ubiquitin travels through the column over more time) could improve future yields. However, the current procedures provide sufficient yield for bioanalytical methods. Purified β-gal and ubiquitin were concentrated to 92 μM and 1.5 mM respectively.

Chapter Three

β-GAL KINETICS BEFORE AND AFTER ENCAPSULATION

Introduction

Coacervate forming biodegradable thermoresponsive polyesters (TR-PEs) are a unique class of potential therapeutic delivery systems. Contrary to nanogel systems, which are typically synthesized as covalently cross-linked micelles[13], TR-PEs are produced as randomly assorted copolymers. After reconstitution of the solid, the polymer's phase is regulated by the LCST. This intrinsic property varies with polymer assortment and concentration. As polymer concentration and molecular weight increase, the LCST decreases. Polymer molecules will form coacervate droplets and be in the 'coacervate' phase if the solution temperature is above the LCST. If the temperature is reduced below the LCST, the TR-PEs will return to the 'soluble' phase and be monomeric within solution. This intrinsic property can be used to control the encapsulation of model protein cargos. TR-PEs can contain modular pendant groups to influence interaction with cargo; modifying the pendant groups could increase or decrease affinity for targeting molecules.[14] Previous research has specifically shown that TR-PEs are hydrolytically degradable at low pH and show low cytotoxicity.[15] The TR-PEs attributes are enticing for potential use as a therapeutic packaging system.

Literature covering TR-PE encapsulation rarely investigates β-gal as a model protein. Proteins like BSA, insulin, and lysozyme are used more commonly to investigate

the encapsulation of protein into TR-PE droplets. These proteins are smaller and provide high loading efficiency.[10] Although β-gal, a 464 kDa homotetramer in the native active state, is quite larger than model proteins typically used for encapsulation studies and may hold a lower loading efficiency, it remains attractive for these studies with its intrinsic enzymatic activity and similar monomer size (116 kDa) to monoclonal antibodies (~150 kDa). β-gal forms an active homotetramer in solution and hydrolyzes β-1,4-galactosidic linkages. This can be used to test the effects of TR-PE encapsulation on the enzymatic activity. Comparing β-gal activity before and after encapsulation provided insight into whether interactions with TR-PEs alter β-gal activity.

When focusing on β-gal enzymology, reaction conditions were chosen to facilitate a coherent analysis with the initial velocity and steady state assumptions to operate at or near V_{max}.[16,17] Chlorophenol Red Galactopyranoside (CPRG) was the indicator molecule used to elucidate β-gal activity before and after encapsulation. β-gal hydrolyzes the β-1,4-galactosidic linkage within CPRG to liberate the chlorophenol red (CPR) moiety. This release increases absorbance at 574 nm and was measured to obtain the maximum velocity (V_{max}) of individual protein samples. Separate from the enzyme assay mixtures, a Bradford total protein assay allowed quantitation of β-gal within the samples.[18] These provided the basis for calculating kinetic parameters, like rate normalized to total protein concentration (R_n), a k_{cat} -like value, and specific activity (SA) (**Equations 1, 2**); to compare the effects of various TR-PEs interacting with β-gal and whether activity had been decreased or retained. The following equations contain a conversion factor obtained from a *G-Biosciences* protocol, which describes CPRG enzymatic assays with β-gal. It

was systemically used in all calculations. This enabled comparison of like values between polymer samples.

Equation 1 $$R_n\ (\mathrm{min}^{-1}) = \text{Reaction Rate}\ \left(\frac{\text{A.U.}}{\text{min}}\right) * \ 0.055(\mu\text{M}) \ / \ [\beta\text{gal}]\ (\mu\text{M})$$

Equation 2

$$[\text{CPR}]\left(\frac{\mu\text{mol}}{\text{L}}\right) = \text{Reaction Rate}\ \left(\frac{\text{A. U.}}{\text{min}}\right) * \text{Experiment Duration (min)} * 0.055\left(\frac{\mu\text{mol}}{\text{L}}\right)$$

$$\mu\text{mol CPR}\ = [\text{CPR}]\left(\frac{\mu\text{mol}}{\text{L}}\right) * \text{Reaction Volume (L)}$$

$$\beta\text{gal Activity (U)} = \ \mu\text{mol CPR} \ / \ \text{Experiment Duration (min)}$$

$$\text{Specific Activity}\ \left(\frac{\text{U}}{\text{mg}}\right) = \ \beta\text{gal Activity (U)} \ / \ \text{Total Protein (mg)}$$

The Bradford assay was used to quantify the total amount β-gal in each sample. As mentioned prior, this was performed separately from the enzymatic assays, with the same samples, and allowed the calculation of retention rates. Retention rates were calculated by dividing the amount of β-gal within sample H by the sum of β-gal measured, with the Bradford, from each sample. This calculation is described in **equation 3**. This calculation does not include β-gal sample not recovered from the initial loading and was shown in (**Appendix 2.3**).

Equation 3 $$\text{Retention rate (\%)} = \frac{\text{Amount of } \beta\text{−gal in sample H (mg)}}{\text{Sum of } \beta\text{−gal in samples H and S1−S4 (mg)}} * 100$$

Multiple polymer variants were screened and evaluated for capturing and preserving this high molecular weight model protein and were examined for their potential future therapeutic packaging applications. The polymer variants, numbered 1 to

7, contained varying pendant group containing units which may have affected affinity for a model protein cargo and could possibly modify the loading potential through droplet size or stability (**Figure 3.1**). Their respective absolute molecular weights and predicted LCST values follow (**Table 3.1**). The molecular weights and pendant group units were expected to influence the corresponding LCSTs. The effects of each polymer's model protein cargo encapsulation were studied to gain insight into the impact of pendant group variation.

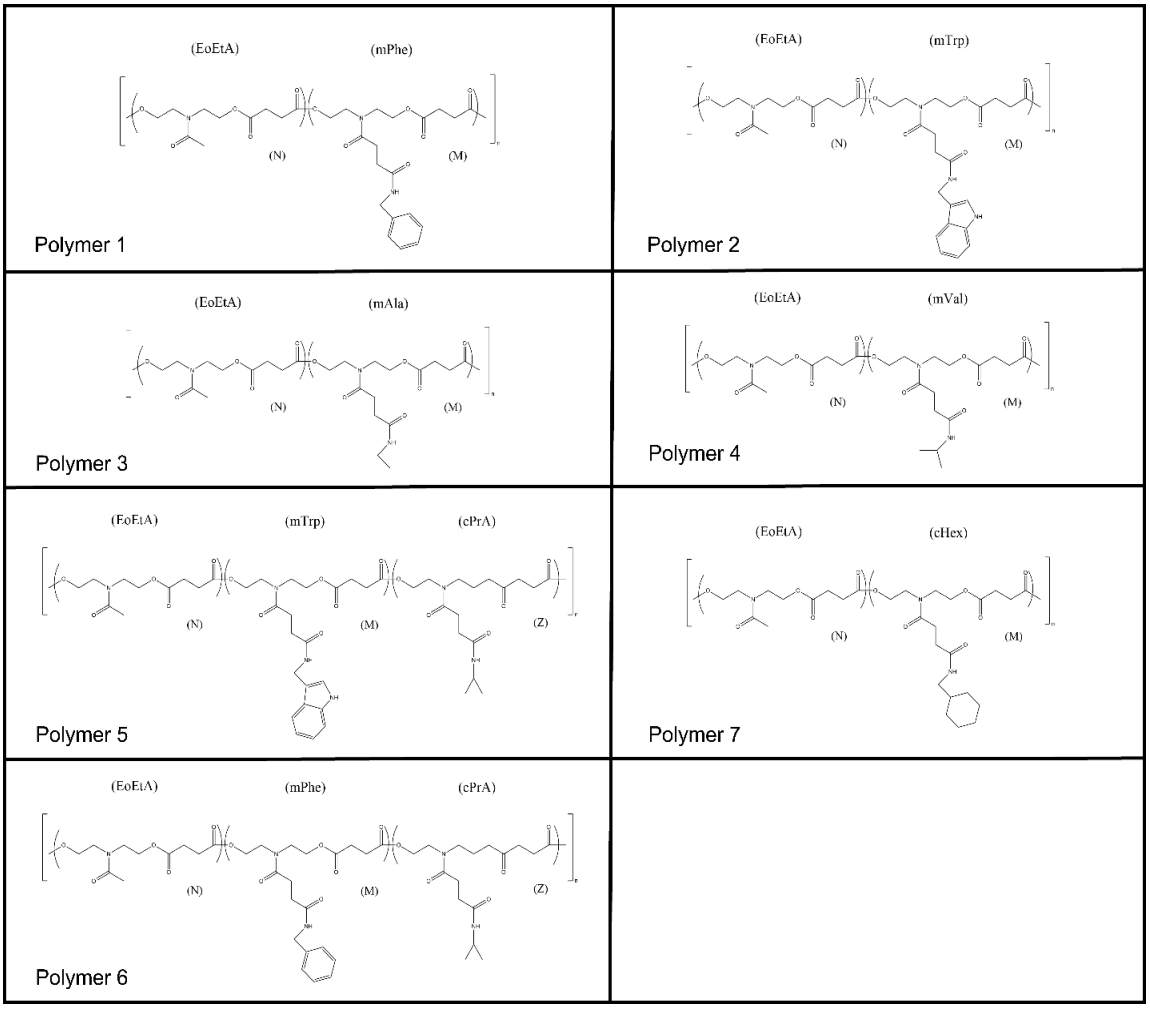

Figure 3.1. Polymer unit structures made with ChemDraw. Monomer unit names are above their respective units within the structure.

Polymer Variants (N:M:[Z])	Absolute molecular weight (kDa)	Predicted LCST [10 mg/mL] (°C)
P1 (EoEtA-mPhe) (85:15)	39.4	9
P2 (EoEtA-mTrp) (90:10)	43.5	8
P3 (EoEtA-mAla) (70:30)	37.5	10
P4 (EoEtA-mVal) (70:30)	34.86	11
P5 (EoEtA-mTrp-cPrA) (90:5:5)	42.49	8
P6 (EoEtA-mPhe-cPrA) (85:10:5)	35.78	10
P7 (EoEtA-cHex) (90:10)	39.44	10

Table 3.1. Polymer variants used within experimentation were described. (N:M:[Z]) represents the respective ratio of monomer unit occurrence within the random copolymer. The absolute molecular weights were calculated upon polymer synthesis. Each polymer's final concentration in assay mixture was 10 mg/mL. The corresponding predicted LCST for 10 mg/mL was included for reference.

Experimental

Coacervate-forming biodegradable TR-PEs were obtained from the Joy Laboratory, University of Akron. A 20 mg/mL polymer stock solution was made by weighing 20 mg of frozen, solid polymer and by adding 1 mL of 1x PBS pH 7.4 buffer. Reconstitution of the polymer required a series of vortexing and placing the polymer sample on ice. The tube containing polymer was vortexed until cloudy and placed on ice. This was repeated until polymer was completely reconstituted into buffer, indicated by a clear solution while on ice. The polymer stock solution was either stored at -20°C or used for encapsulation assays.

The encapsulation process is outlined in **Appendix 2.1**. β-gal for encapsulation kinetics assays was produced in-house as previously mentioned in Chapter 2. Combine equal parts of ~20 μM β-gal and 20 mg/mL polymer in an Eppendorf tube on ice, this is the harvest sample "H". Sample H was placed in a tube rack at room temperature (RT) to allow coacervation of polymer. Once fully within the coacervate phase, the sample was returned to ice until polymer returned to the aqueous phase. The sample was returned to the tube rack for coacervation to occur. This repetition encouraged interactions between protein and polymer.

After droplets formed and the sample was opaque (**Appendix 2.1**), sample H was centrifuged at 4000xg rcf for 1.5 minutes at RT. A pellet was formed and supernatant was siphoned by pipette into a separate tube; this was sample "S1" and was withheld at RT. Buffer, of equal volume to the original sample H, was injected at RT into sample H in a fashion to disturb and resuspend, but not dismantle, the polymer pellet. Centrifugation was repeated with the same parameters. The supernatant was siphoned from the pellet once more and withheld in a separate tube at RT; this was the first wash step, and the sample was denoted as sample "S2". Two more identical wash steps were conducted to obtain samples "S3" and "S4". Finally, buffer of equal volume was added to sample H to disrupt the pellet. Sample H was placed on ice to encourage polymer to return to the aqueous phase.

A kinetic assay with the following parameters was conducted: kinetic assay, one point absorbance (574 nm), 30-minute experiment duration with 20-second read intervals, and a 3 second medium orbital shake. A 96-well black, clear bottom microplate was prepared at RT with 200 uL of 1 mM CPRG in all wells simultaneously being used for

kinetics assay. Samples of purified β-gal were created by serial dilution series for a standard curve. Samples S1-4 were aligned to their respective well coordinates within a tube rack and sample H was retained on ice. 10 uL of samples were added accordingly to their planned well locations. The microplate was inserted into the reader and the kinetic assay was started. Data was collected and analyzed after completion to obtain kinetic information. A standard operating protocol for this reconstitution and encapsulation process was included (**Appendix 2.1**).

A total protein assay was conducted with Bradford reagent in a 96-well black, clear bottom microplate. Bradford reagent was inverted to gently mix and 200 uL was added to planned wells at RT. Serially diluted β-gal, from 4 mg/mL to 25 ug/mL, determined by A_{280}, formed a standard curve. Samples H, on ice, and S1-4, at RT, were prepared from encapsulation studies and 25 uL were added to their respective wells. Each well is gently mixed to efficiently distribute the sample within reagent. The plate was incubated at RT for 30 minutes. An endpoint read assay was programmed into a plate reader to measure the absorbance of the samples at 595 nm. Data was collected and analyzed to obtain a ug/mL concentration of protein present within sample, which was used to calculate the amount of β-gal in milligrams.

While creating standard curve data for both the kinetics and total protein assays, a negative control was included with a well only containing respective reagent and buffer. The negative control for testing any samples with polymer present required a pure polymer sample. These were created by adding 10 mg/mL polymer samples into reagent solution to mimic the maximum amount of polymer present within samples. The

absorbances from the negative controls were subtracted from a given sample's absorbance.

Results

The optimization of initial encapsulation kinetic assay parameters concerning polymer concentration, substrate concentration, and β-gal concentration were critical to provide useful data. Polymer 1 was reconstituted to varying concentrations (5, 10, 20 mg/mL) and 20 mg/mL chosen for subsequent assays. Although the relatively high concentration of polymer was tricky to reconstitute, multiple freeze-thaw cycles improved polymer solubility. These cycles allowed the disbandment of solid polymer and encouraged polymer to enter the aqueous phase upon being thawed. Substrate, CPRG, concentration was assayed with a serial dilution and 1 mM was chosen as it provided linear velocities for the expected low β-gal concentrations. After the previous parameters were determined, β-gal concentration was explored for droplet loading potential. It was assumed that not all β-gal present in solution with polymer would be encapsulated, therefore, initial β-gal loading concentrations around 20 μM were decided to be most effective to observe measurable enzymatic activity and to remain within the Bradford assay's limit of detection (LOD), calculated to be 27.2 μg/mL using a standard curve (**Appendix 2.2**).

An important consideration for initial assay parameters was the potential for polymer coacervation within the plate assays. This would have caused optical scattering and interference of the colorimetric assays. It was initially thought that coacervation

would occur within the plate assays. However, this was unlikely due to a polymer concentration well below the amount to permit coacervation. As previously mentioned, the intrinsic LCST property scales oppositely with polymer concentration. A low concentration would result with a high LCST, much higher than the temperature used during plate reading. The final concentration of polymer within a well is maximally 0.5 mg/mL. Therefore, the LCST threshold to form droplets within a given well was not attainable.

It is important to visualize where the protein is within the samples. When protein and polymer are combined on ice, sample H, they are both aqueous together and can freely diffuse. When moved to RT, polymer will enter the coacervate phase and form droplets, encapsulating protein. There will still be protein that is not captured within solution while some will be in the droplets. In addition, miniscule amount of polymer will remain in aqueous phase after the coacervation reaches its equilibrium. After centrifugation step one, protein that is captured will be within droplets in the pellet and free protein will be within solution. The subsequent wash steps are necessary to ensure that any protein caught interstitial between droplets are diluted to prevent interference with kinetic assays that follow. At this stage, it is important to gently wash the pellet to minimize possible destruction of the droplets. Although it is possible that some polymer will also be solubilized from the coacervate phase, this was found to be miniscule; visual scattering of coacervation was minimally observed in S1 and not observed within samples S2, 3, and 4. Following the wash steps, the pellet in sample H should be resuspended with the goal of disrupting the droplets from each other and placed on ice to

encourage polymer to return to monomeric units within the aqueous phase, releasing captured protein into solution.

When analyzing the effects of TR-PE encapsulation on β-gal, sample H and sample S4 were compared. This was reasonable due to these final samples were of equal dilution if β-gal was not captured. The combination of enzymatic and total protein assays provided the following possible interpretations of polymer encapsulation, summarized in **Table 3.2**. If TR-PEs did not capture β-gal, it was expected that sample H CPRG activity would equal that the respective sample S4 and sample H signal would be below the Bradford assay's LOD. If TR-PEs captured β-gal but negatively impacted protein integrity, samples H and S4 CPRG activity would be similar and sample H would be within the Bradford LOD; sample H's specific activity would be less than sample S4's SA. If TR-PEs captured β-gal and released active enzyme, sample H's CPRG activity was expected to be greater than sample S4 and would be within the Bradford LOD; sample H's SA would be greater than sample S4's SA.

Assay Type	Possible Interpretations		
	Not Captured	Captured, Activity Altered	Captured, Activity Preserved
Kinetic	H = S4	H = S4	H > S4
Bradford	Below LOD	Within LOD	Within LOD
SA	n/a	H < S4	H > S4

Table 3.2. The conditions for data interpretation of a given encapsulation assay. 'Kinetic' refers to the CPRG colorimetric assay for determining a sample's kinetic characteristics. 'Bradford' refers to the colorimetric total protein quantitation assay, independent of activity. 'SA' refers to a calculated specific activity using information from the previous assays.

TR-PE encapsulation of β-gal (23 μM) with polymer 1 (EoEtA-mPhe) (20 mg/mL) showed sample H CPRG activity greater than S4 within kinetic assays (**Figure 3.2.A**). This represented presence of active β-gal after the encapsulation and wash procedure. Polymer 1 retained 14.1% of β-gal in the coacervate droplets. Sample H had a total protein concentration of 110.7 ug/mL and was detected within the LOD for a Bradford assay (**Figure 3.3.A**). Sample H calculated R_n and SA were calculated as higher than sample S4 (**Table 3.3**). This indicated that polymer 1 encapsulated and released active β-gal.

Polymer Samples		R_n (nM/min)		Specific Activity (U/mg) or (μmol/min/mg)	
Variant	β-gal Retention (%)	H	S4	H	S4
P1 (EoEtA-mPhe)	14.1	0.613	0.597	4.44E-06	4.33E-06
P2 (EoEtA-mTrp)	30.3	0.265	4.723	1.92E-06	3.42E-05
P3 (EoEtA-mAla)	10.8	2.109	0.770	1.53E-05	5.57E-06
P4 (EoEtA-mVal)	18.3	0.234	0.745	1.69E-06	5.40E-06
P5 (EoEtA-mTrp-cPrA)	7.0	0.506	0.394	3.67E-06	2.85E-06
P6 (EoEtA-mPhe-cPrA	19.7	0.380	0.253	2.75E-06	1.83E-06
P7 (EoEtA-cHex)	21.7	0.259	0.622	1.88E-06	4.51E-06

Table 3.3. Calculated values of R_n and SA for each β-gal encapsulation assay with individual polymer sample and their respective H and S4 samples.

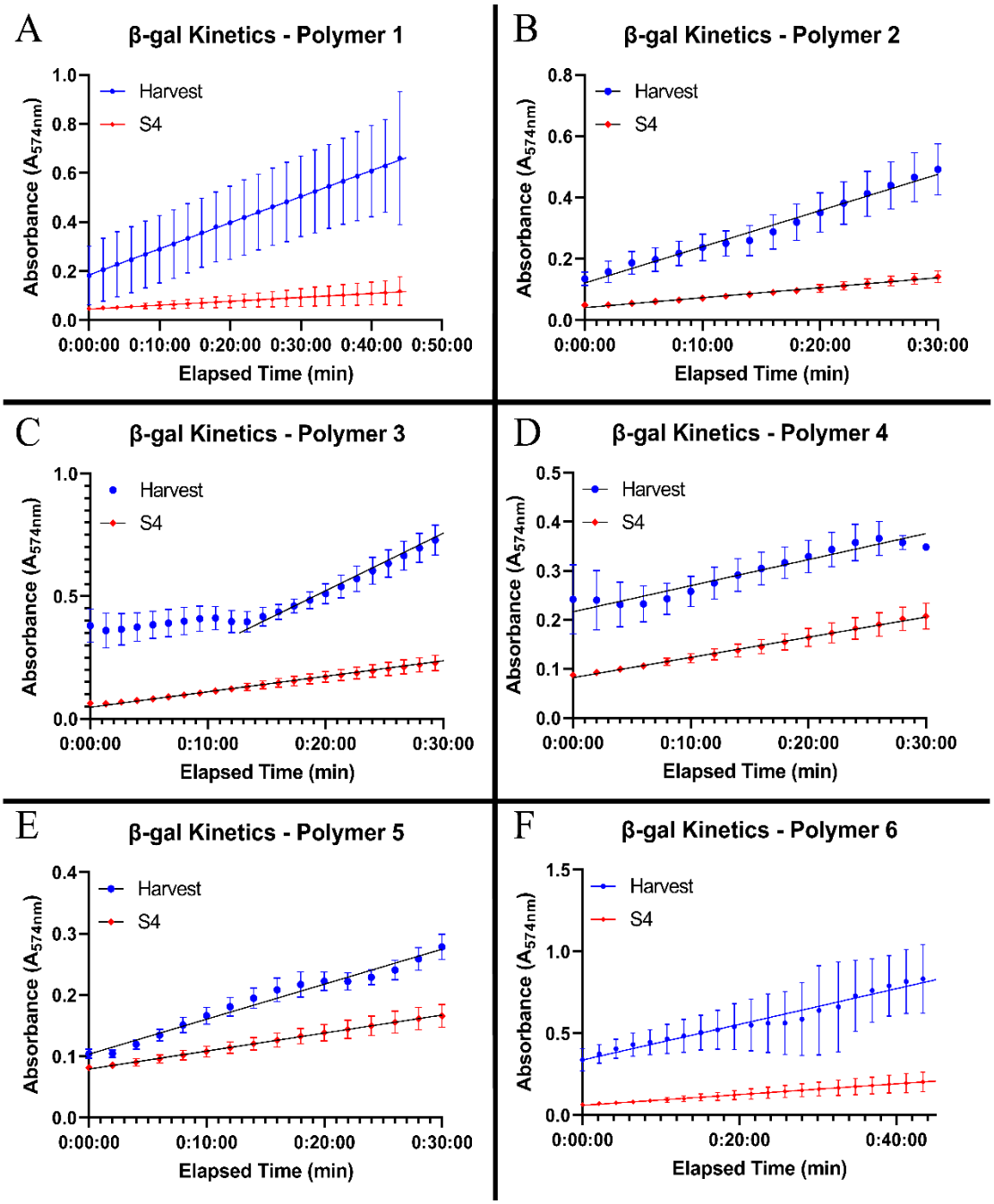

Figure 3.2. β-gal enzymatic assays after encapsulation with polymers 1 through 6 (20 mg/mL) and β-gal (23 μM). The generation of CPR product from CPRG substrate (1 mM) observed at A_{574nm} through either 30 or 45 minutes at RT. Note: panel C line of best fit after 12 minutes due to artifact.

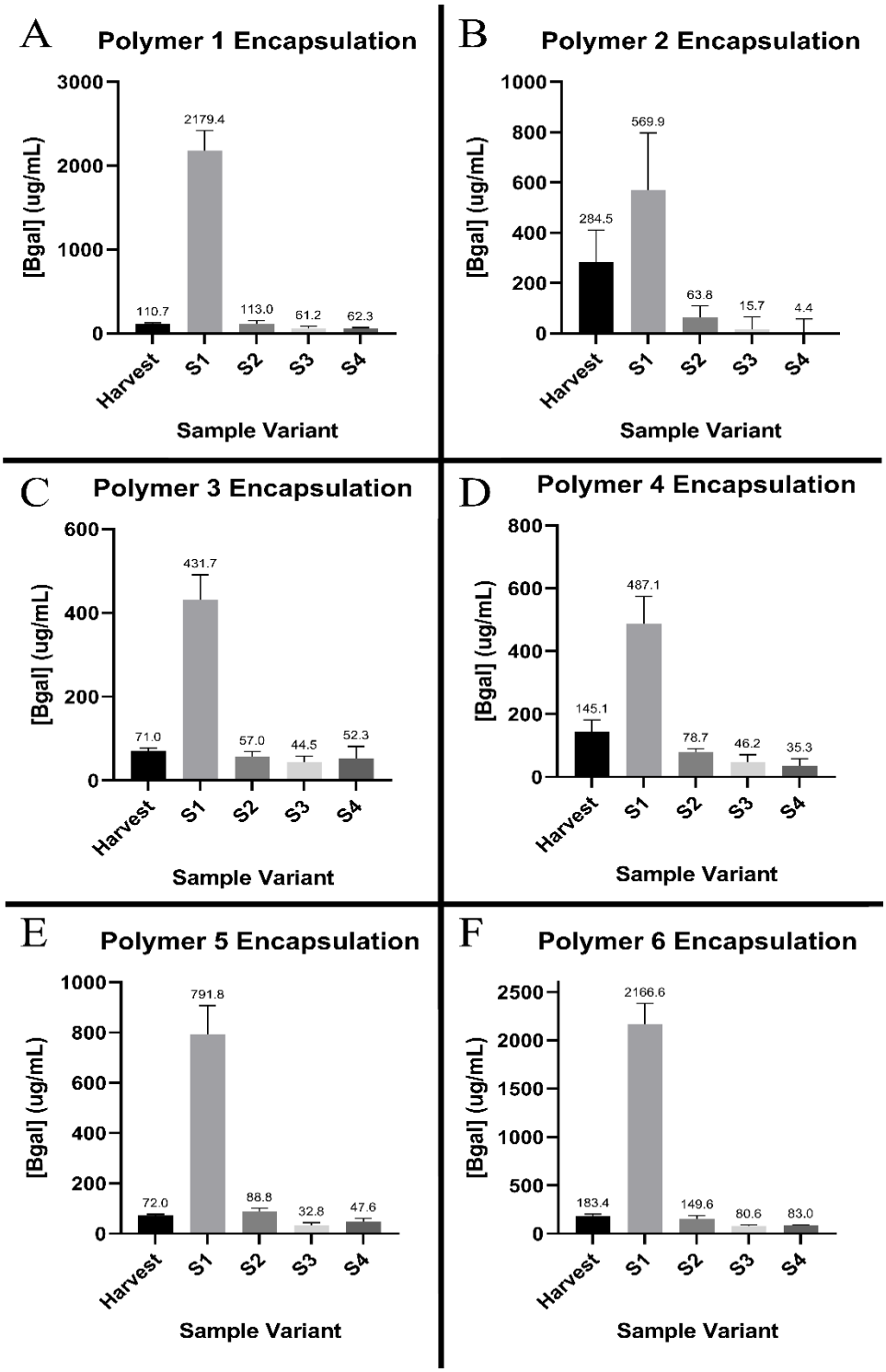

Figure 3.3. Total protein concentration quantitation assay corresponding to various β-gal encapsulation samples. After 30-minute incubation with Bradford reagent at RT, samples were analyzed with an endpoint read at 595 nm.

Encapsulation of β-gal (23 μM) with polymer 2 (EoEtA-mTrp) (20 mg/mL) demonstrated sample H activity greater than S4 within kinetic assays (**Figure 3.2.B**). This suggested active β-gal was present after encapsulation and release. Polymer 2 provided a 30% retention of β-gal within droplets. A total protein concentration of 284.5 ug/mL in sample H remained well within the LOD for a Bradford assay and was significantly greater than samples S2-4 (**Figure 3.3.B**). The R_n and SA were calculated to be significantly lower than sample S4 (**Table 3.3**). These data indicated that β-gal accreted within coacervate droplets, but its integrity was compromised. It is notable to mention that samples S3 and S4 were not within the LOD for the Bradford assay. This might have skewed the conclusions and inflated the R_n and SA calculations.

It was hypothesized that polymer 2, with the pseudo tryptophan pendant group, would have higher association affinity for proteins. This was confirmed when the calculated retention rate was greater than the other examined TR-PEs (**Table 3.3**). The inclusion of the pseudo tryptophan pendant group may be interacting 'too much' with β-gal and reducing the protein's integrity and thus, its activity. It is possible that the semi-conjugated unit interacted with β-gal residues near the active site or even the binding interface between subunits which would have prevented formation of the active β-gal homotetramer. A simpler theory was that the high local concentration of β-gal could result in aggregation when in coacervate droplets or within an environment of decreased solvent interactions.

Encapsulation analysis of β-gal (23 μM) with polymer 3 (EoEtA-mAla) (20 mg/mL) provided a greater activity for CPRG than sample S4 (**Figure 3.2.C**); active β-gal was present within the harvest sample. Polymer 3 retained 71.0 ug/mL β-gal, 10.8%

of the total recovered protein and within the LOD (**Figure 3.3.C**). The R_n and SA for sample H were calculated to be greater than S4 (**Table 3.3**). This suggested that polymer 3 captured β-gal within droplets and released active enzyme.

Encapsulation of β-gal (23 μM) with polymer 4 (EoEtA-mVal) (20 mg/mL) exhibited similar results as polymer 2. Sample H activity was similar to S4 within kinetic assays (**Figure 3.2.D**). Polymer 4 retained approximately 18% of recovered β-gal. With a total protein concentration within the LOD, 145.1 ug/mL, protein was withheld from the subsequent wash steps S2-4 (**Figure 3.3.D**). The R_n and SA for β-gal encapsulated by polymer 4 were calculated to be lower than the corresponding S4 sample (**Table 3.3**). Current data suggested that although polymer 4 retained β-gal, its integrity was altered through the encapsulation process.

β-gal experienced negative effects within the encapsulation and release process of polymer 4. This resulted with a relatively decreased SA and were explained with similar theories previously mentioned of a higher local concentration of β-gal causing aggregation, thus, lowered SA. However, polymer 4 contains a pseudo valine pendant group within the copolymer design. This was significantly different than a pseudo tryptophan group. With the assumption that valine pendant groups were not to be reactive with surface β-gal residues, it may be possible that the monomer unit, (EoEtA), within all polymers and responsible for LCST properties, was the source of minor interference for β-gal activity. This unit could have interacted with the accessible active site residues or β-gal monomer-monomer binding interfaces.

Encapsulation experimentation on β-gal (23 μM) with polymer 5 (EoEtA-mTrp-cPrA) (20 mg/mL) demonstrated similar effects on protein integrity as polymer 1. β-gal

activity within the CPRG assay was greater than the respective S4 sample (**Figure 3.2.E**). Total protein concentration within sample H was 72.0 ug/mL, this was within the LOD (**Figure 3.3.E**). Polymer 5 retained 7% of the recovered β-gal. The R_n and SA properties for β-gal within sample H were calculated to be greater than sample S4 (**Table 3.3**). These data suggested that the active β-gal was captured and released.

Encapsulation experiments with polymer 6 (EoEtA-mPhe-cPrA) (20 mg/mL) and β-gal (23 μM) showed that sample H held higher CPRG activity relative to S4 (**Figure 3.2.F**). Total protein concentration analysis displayed polymer 6 encapsulated β-gal to 183.4 ug/mL; a 19.7% protein retention rate for measured (A_{280}) protein present within all samples (**Figure 3.3.F**). This measurement was within the Bradford LOD. The R_n and SA for sample H were greater than the related sample S4 (**Table 3.3**). This indicated that β-gal was encapsulated by polymer 6 and its activity was retained. The larger error bars after experimental $time_{20:00}$ were likely sourced from various retention rates between individual encapsulation experiments.

The data analyses for encapsulation and release experiments of β-gal with polymer 7 were included within **Appendix 2.4**. The data were not included in the main text because of similarity to polymer 2 results. Briefly, polymer 7 encapsulated β-gal with a 21.7% retention rate but influenced a decrease in R_n and SA (**Table 3.3**).

Error bars within kinetic assay analysis were typically larger for harvest samples relative to the supernatant samples. This was interpreted to occur due to non-specific coordination of TR-PEs to protein and was shown by the variance of kinetic data within harvest samples and the chemical shift perturbation evidence within nuclear magnetic resonance experiments with ubiquitin (**Chapter 5**). It was hypothesized that TR-PEs

formed non-uniform volume coacervates, therefore the loading capacity/efficiency fluctuated between individual polymer samples. This suggested that these polymers followed a random encapsulation dynamic.

These data suggested that β-gal was captured within various TR-PEs and active β-gal was released. This demonstrated that coacervate-forming TR-PEs can encapsulate and release a large target protein, which has not been previously shown. Experimentation with polymers 2, 4, and 7 exhibited high retention rates but showed negative effects on released β-gal activity. Encapsulation and release with polymers 1, 3, 5, and 6 showed varying retention rates and demonstrated active β-gal was released from the droplets.

Subsequent chapters will provide confirmation that these studies are representative of encapsulated β-gal with fluorescence and investigate how TR-PEs interact with ubiquitin on a biophysical level with nuclear magnetic resonance.

Chapter Four

ENCAPSULATION STUDIES WITH FLUORESCENTLY LABELED MODEL PROTEIN CARGOS

Introduction

Fluorescence microscopy is a technique where fluorescently labelled target molecules are studied at the microscopic level. Fluorescence provides high sensitivity and specificity by illuminating the analyte with the fluorophore's excitation wavelength and receiving its emission spectrum. Fluorescence microscopy is commonly used to study interactions within cellular systems, however it can also be utilized to study individual small molecule systems.

Confocal fluorescence microscopy (CFM) holds similar principles to fluorescence microscopy in using fluorescence to study analytes. Instead of a traditional widefield microscope, a confocal microscope is equipped with fluorescent filters. The confocal microscope focuses the laser to a specific depth within samples which leads to the emission of light directly at that depth. CFM is used to generate three-dimensional images by collecting fluorescent data from multiple focal planes to form a z-stack. This technique was specifically used in the following experimentation to examine TR-PE encapsulation of fluorescently labeled β-gal.

Fluorescein isothiocyanate (FITC) was originally used in antibody labeling.[19] When labeling protein, the isothiocyanate group within FITC reacts with the N-terminal residue's α-amino group below pH 9.0. Increasing labeling efficiency requires the reaction to be above pH 9.0; this enables deprotonation of ε-amino groups belonging to surface lysine residues which will react with the ITC group.[20]

Experimental

β-gal stock was diluted to 23 μM (2.67 mg/mL) with 0.1 M sodium bicarbonate pH 9.0. FITC was dissolved in anhydrous dimethylformamide to 10 mg/mL. While mixing β-gal, 100 uL of FITC solution was added. This solution was incubated for 1 hour at RT with slight mixing. Sample was desalted with a 5 mL 7K MWCO spin desalting column at 1000 rcf. FITC-β-gal was eluted from the column with 1x PBS pH 7.4 with a final concentration of 17.8 μM via NanoDrop™.

FITC-β-gal endured the encapsulation and washing process with each polymer variant as previously described (**Chapter 3)** with one difference. The harvest sample containing FITC-β-gal was not returned to ice at any point after the initial encapsulation, and the pellet was disturbed with 1x PBS pH 7.4 to resuspend droplets to the original volume amount. Final concentrations for FITC-β-gal and a given polymer variant were 8.9 μM and 10 mg/mL respectively. Individual samples were diluted by ¼ with 1x PBS pH 7.4 and were pipetted into a chamber slide system. A Zeiss LSM 700 Laser Scanning Confocal Microscope, equipped with a FITC filter, produced z-stack images at 40x

magnification. Experimental controls included FITC-β-gal and a polymer sample with the same applied dilutions.

Results

CFM data was beneficial to obtain for FITC-β-gal. This allowed visualization of fluorescently labeled β-gal within coacervate droplets and comparison to encapsulation data obtained previously (**Chapter 3**). It was important to realize that only FITC-β-gal was visualized with CFM. Polymer samples do not emit fluorescent light at FITC emission wavelength, 516 nm. Therefore, any specifically localized fluorescent signals were inferred to be FITC-β-gal captured within a given coacervate droplet.

Protein-FITC labeling was concentration dependent, which required a protein concentration between 2 and 10 mg/mL. β-gal, 23 μM or 2.67 mg/mL, was used for FITC labelling and provided a final FITC-β-gal concentration of 17.8 μM (2.07 mg/mL). Although there was some loss of protein (likely to desalting), this concentration was acceptable for fluorescence assays.

CFM assays required miniscule protocol optimizations, which simply included exploration of sample dilution to obtain clear images of droplets and determining what slide-type should images be collected in. A pilot experiment showed that initial samples depict highly dense droplet formations after proceeding through the encapsulation-wash method. The pilot samples with encapsulated FITC-β-gal were serially diluted by ½ and examined with CFM. It was determined that a ¼ dilution was sufficient to provide resolved images of captured FITC-β-gal. The CFM image of FITC-β-gal encapsulated

with polymer 5 was obtained with a 1/8 dilution to specifically locate the one larger droplet (**Figure 4.2.E**).

The experimental controls included the positive of pure FITC-β-gal and the negative pure polymer sample with dilution equal to analytes. They were not included in the text due to a solid green, fluorescent image within the positive control and a pure black image within the negative control.

The typical glass cover slide and a chambered slide were explored for image collection. The initial CFM assays with FITC-β-gal were conducted in glass cover slides (**Figure 4.1**). TR-PEs were suspected to form spherically shaped coacervate droplets, as this would be the thermodynamically stable conformation within solution. Glass cover slide assays depicted TR-PEs as oblong shaped droplets, providing information that the droplets may act as physical barriers and adapted to the glass cover slide compression. This was not directly problematic; however, it was preferred to analyze coacervate droplets containing FITC-β-gal within a less-physically constrained environment. For subsequent experimentation, chambered slides were used to analyze sample.

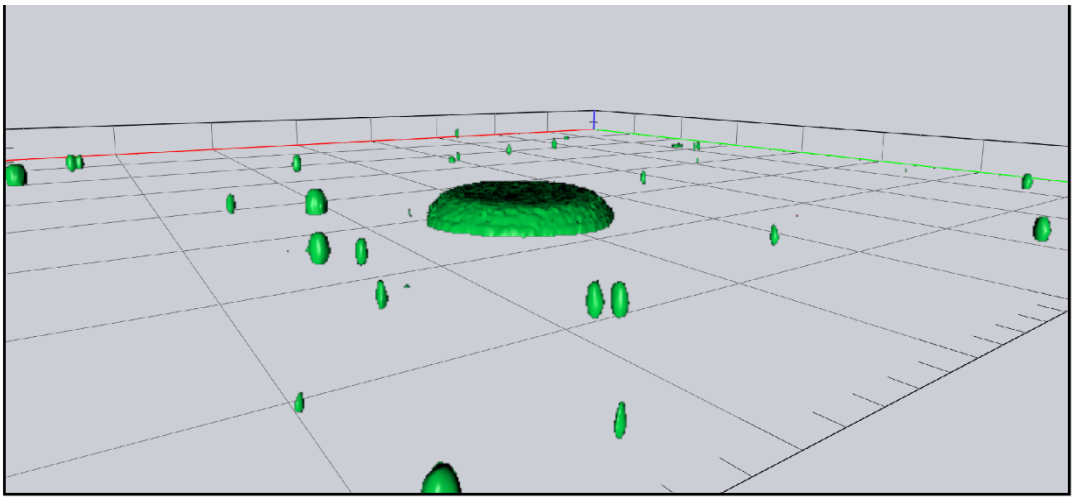

Figure 4.1. Three-dimensional CFM image (40x magnification, FITC filter) of FITC-β-gal (17.8 μM in 1x PBS pH 7.4) and encapsulated with polymer 6 (EoEtA-mPhe-cPrA) (20 mg/mL in 1x PBS pH 7.4). Sample was analyzed on a glass cover slide.

Encapsulation experiments on FITC-β-gal with TR-PEs demonstrated that FITC-β-gal was localized after polymer treatment and was signified by localized fluorescence signals (**Figure 4.2**). This interpretation expressed that TR-PEs do capture the protein. Occasionally, there was instance of non-uniform fluorescence signal within a given droplet. This suggested that some FITC-β-gal was aggregated while encapsulated within droplets, which may be caused by local concentrations above the solubility limit of this large protein. These fluorescent spikes were not visualized within the positive control image. Polymer variants also exhibited varying coacervate droplet sizes within CFM and were summarized (**Table 4.1**).

Polymer Sample	β-gal Retention (%)	Average Diameter (μm)	Standard Deviation (μm)
P1 (EoEtA-mPhe)	14.1	4	1.2
P2 (EoEtA-mTrp)	30.3	6	2.1
P3 (EoEtA-mAla)	10.8	2.5	0.8
P4 (EoEtA-mVal)	18.3	3	2.3*
P5 (EoEtA-mTrp-cPrA)	7.0	4	1.1*
P6 (EoEtA-mPhe-cPrA)	19.7	4	0.9
P7 (EoEtA-cHex)	21.7	5	3.7

Table 4.1. Table of polymer sample descriptions and characteristics within CFM assays. (*) Polymer 4 and 5 outliers were not included in the standard deviation calculation; the large signal formations were not observed elsewhere within the samples.

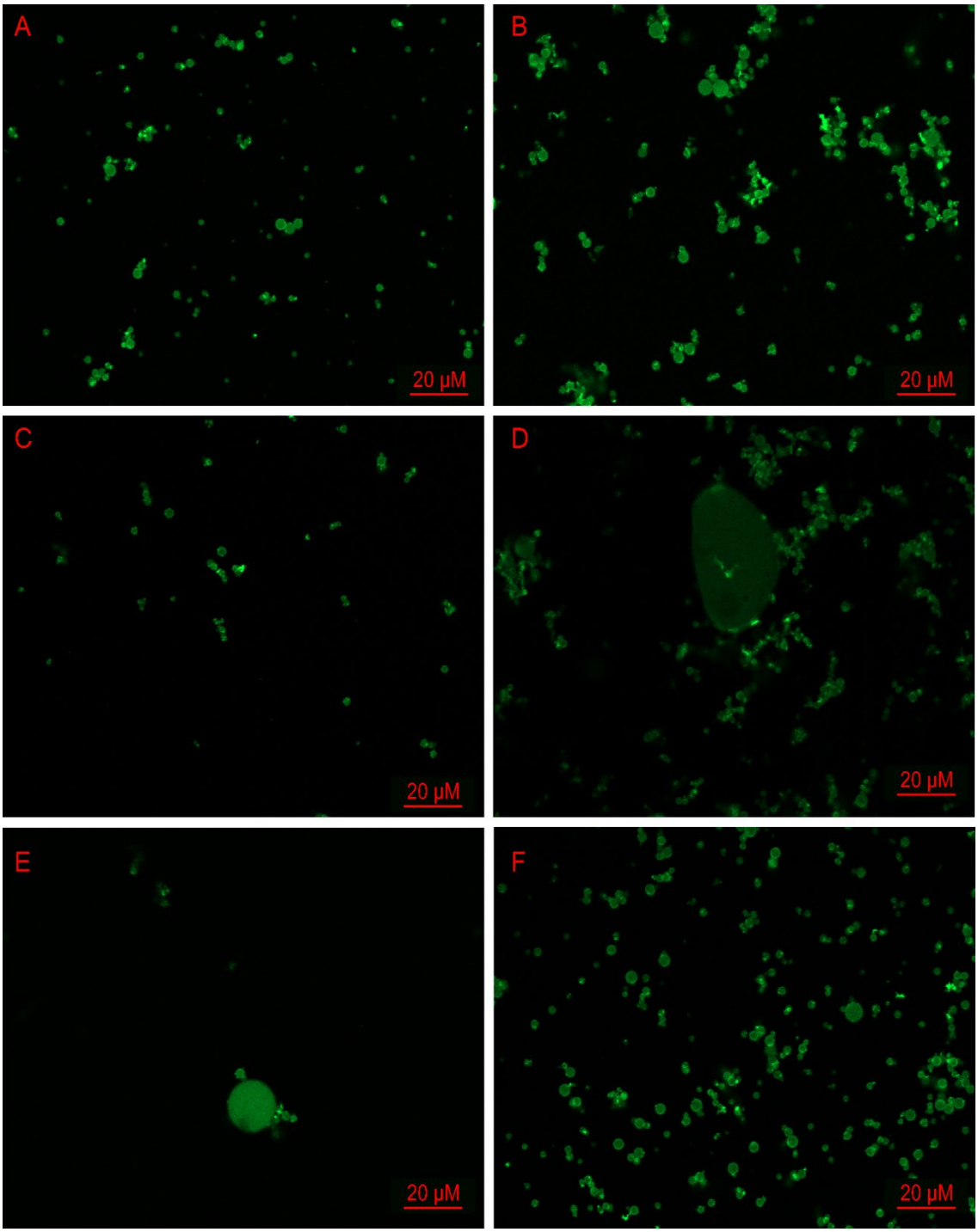

Figure 4.2. Two dimensional CFM images (40x magnification, FITC filter) of FITC-β-gal (17.8 μM in 1x PBS pH 7.4) and encapsulated in various TR-PEs (20 mg/mL in 1x PBS pH 7.4) (**Figure 3.1**). FITC-β-gal was visibly localized within spherical volumes,

assumed to be contained within coacervate droplets. (**A**) FITC-β-gal localization when combined with polymer 1. (**B**) Containment upon polymer 2 treatment. (**C**) FITC-β-gal localized within polymer 3; showed physically smaller droplets relative to other TR-PEs. (**D**) Encapsulation with polymer 4 showed fluorescent localization. Wide signal received from the image center. Polymer 5 encapsulation of FITC-β-gal showed a larger singular spherical fluorescent signal relative to other TR-PEs. (**F**) FITC-β-gal signal localized by polymer 6 encapsulation. **Note**: 2D CFM image of polymer 7 (**Appendix 3.1**).

Various encapsulation experiments of FITC-β-gal remained generally similar, besides the differing ranges of droplet size. This remained as useful information concerning the characterization of polymers and their respective pendant groups. Polymers 5 and 6 both contain monomer units with a -cPrA- pendant group (**Figure 3.1**). This pendant group was previously suggested to aid in larger coacervate droplet formations and more uniform droplet size to capture a higher concentration of targeted cargos. CFM data analyses indicated this to be true to an extent. Comparison of the two polymers showed similar average droplet sizes and standard deviations; the -cPrA- pendant groups might be useful in forming more uniformly distributed droplet sizes. However, these analyses were limited to samples sizes only imaged on the confocal. A more accurate analysis should be conducted with flow cytometry to confirm this proposition.

Although amounts of FITC-β-gal were suspected to be aggregated, TR-PEs encapsulated and retained FITC-β-gal through the harvest washing process; this highlights TR-PEs structural resilience when exposed to the external washing forces. The

TR-PEs also formed a range of coacervate droplet sizes; this was beneficial to further explore the optimization of droplet size in relation to protein encapsulation.

Chapter Five

NUCLEAR MAGNETIC RESONANCE WITH UBIQUITIN AND TR-PES

Introduction

Nuclear magnetic resonance (NMR) is a non-destructive advanced multidisciplinary characterization technique. NMR functions by magnetizing a spin active nucleus, like ^{1}H, and uniformly orients its spin states. A radio frequency pulse is applied to excite the nuclei. The relaxation signal of the excited nuclei is received, processed with a Fourier transform, and represented as a resonance within a spectrum. Traditionally, NMR was constrained to one-dimensional ^{1}H NMR and most effective on small molecules.[21] Today, two- and three-dimensional NMR is effectively used with the inclusion of additional spin active nuclei like ^{13}C and ^{15}N. Isotopic labeling of expressed and purified proteins enables robust application for biophysical analysis of protein structure and integrity.[22]

Saturation transfer difference (STD) NMR was previously used to investigate TR-PE interactions with model protein cargos like doxorubicin. This type of experiment focuses on various chemically different ^{1}H groups to detect transient interactions, in this case, between polymer and protein.[23] Although this method is effective for determining the existence of a set of interactions, a method is required to specifically describe where those interactions occur on the protein.

Heteronuclear single quantum coherence (HSQC) experiments are fundamental to protein NMR and can provide further insight concerning TR-PE and protein interactions. HSQCs are frequently used as a fingerprinting analysis method. When isotopically labelling protein with ^{15}N, experiments will provide resonances, or signals, corresponding to a specific residues' back-bone amide. These resonances can be compared between a reference sample, pure protein, and the experimental samples. That comparison aids with visualizing chemical environment changes at those specific residues within the target protein. Change in chemical environment is indicated when a certain resonance undergoes a chemical shift perturbation (CSP), broadening (CSB), or sharpening (CSS) event. CSP is marked by an altered chemical shift in ^{1}H, ^{15}N, or both dimensions and is indicative of binding or association. CSB is depicted by a decreased signal intensity, whereas CSS is visualized with increased signal intensity; these events generally indicate chemical environment change. All events are critical to answering the question of 'how' TR-PEs may be interacting with protein.

Ubiquitin was chosen to elucidate the effects of TR-PEs on protein structure and integrity for the ability to control its expression and purification with ^{15}N-labelled ammonium chloride and low molecular weight (8.6 kDa). The low molecular weight holds two main benefits: efficient NMR capability at low concentrations and similar size to therapeutics like insulin (5.8 kDa). These characteristics make ubiquitin an ideal model protein cargo for TR-PE studies.

Variable temperature NMR (VT-NMR) is critical for analyzing the interactions between ubiquitin and TR-PEs. It is supposed that TR-PE pendant groups encourage accumulation of ubiquitin within the coacervate droplets. Modulating the temperature of

the sample prior to an experiment will dictate if TR-PEs are within the aqueous or coacervate phase, based on an individual polymer's LCST. This will allow investigation into ubiquitin and polymer interaction when both are aqueous and then when polymer enters the coacervate phase. Analyzing CSP, CSB, and CSS events of specific ubiquitin residues at these stages of droplet formation will provide conclusion if various pendant groups interact differently with ubiquitin to encourage encapsulation.

Experimental

Sample preparation began with combination of TR-PE sample (**Table 3.1**), ^{15}N ubiquitin, and D_2O (*Cambridge Isotope Labs*) on ice. The final concentrations within sample were 10 mg/mL, 100 μM, and 8 % (v/v) respectively. A Pasteur pipette was cooled to 4°C to transfer sample into an NMR tube on ice. VT-NMR (Bruker Ascend^{TM} 600 MHz NMR) was conducted at temperatures 5°C, 25°C, and 45°C. Sample was ejected from the probe prior to temperature change. Once the temperature equilibrated, sample was injected into the probe, the magnet was shimmed, and the probe was tuned. Spectra were acquired with 128 scans with an acquisition time of 41.6 ms (^{15}N) / 42.2 ms (^{1}H) and a relaxation delay 469.72 μs. Experiments were conducted with a ^{15}N TROSY-HSQC pulse program with water suppression (**Appendix 4.1**). After spectra acquisition, they were corrected in both dimensions with automatic phase correction followed by manual zero and first order phase corrections. Spectra analyzed within NMRFAM SPARKY software enabled comparisons between the various ubiquitin-polymer samples.

Control experiments included an individual ^{15}N ubiquitin reference as a positive control and a pure polymer 2 reference as a negative control. The controls were generated through the same process as the experimental samples, however, 1x PBS pH 7.4 replaced the corresponding absent component in each sample. Sample acquisition, processing, and analysis followed the same protocol as previously mentioned.

Results

Determination of final analyte concentrations required thorough optimization to provide sensible results. Final ^{15}N ubiquitin concentrations of 50, 100, and 500 μM were examined for their effectiveness with VT-NMR. The final concentration 100 μM provided high resolution for reference spectra (**Appendix 4.2**) at the various temperatures where available residues were assigned and where any 'free' ubiquitin signal outside of a polymer enriched chemical environment was minimized. This concentration would be problematic in traditional protein NMR. However, ubiquitin NMR characterization was robust. Its small molecular weight allowed the protein to tumble more quickly within solution and its corresponding relaxation time, T2, was elongated relative to larger proteins. This allowed sufficient instrument sensitivity and spectra resolution.

The final polymer concentrations of 1, 5, and 10 mg/mL were initially tested for their effects on ^{15}N ubiquitin. Based on preliminary assays, it was determined that polymer at 10 mg/mL demonstrated maximized protein-polymer interactions and was chosen for subsequent analysis. Average polymer concentrations were 2.5 times greater than ubiquitin. Physically, there was approximately 430 ug ^{15}N ubiquitin and 5 mg of

polymer within sample. The difference in total mass within sample suggested an assumption that nearly all ubiquitin was within chemical environment with polymer units.

Experimental conditions and procedures were also optimized. Overall, this pulse program allowed improved protein residue resolution and of resonance near the water line. It was important that sample generation was performed and retained on ice until injecting sample into the NMR probe. At 10 mg/mL, all polymer samples' LCST was between 8-11°C and rapidly entered the coacervate phase at RT. Maintenance of polymer within aqueous phase dictated that a given sample, Pasteur transfer pipette, and NMR tube remain on ice. This allowed confidence that protein-monomer interaction was studied within the VT-NMR experiments at 5°C. Furthermore, experimentation at temperatures 25°C and 45°C elucidated the polymer effects at RT and under heated conditions. These provided information on protein-polymer interaction at a condition where coacervate droplets should be formed and where it was ensured that coacervate droplets were present.

Contrary to the encapsulation kinetics experiments within Chapter 3, the ^{15}N ubiquitin-polymer samples did not undergo the encapsulation and washing procedure. The intention was to analyze various pendant groups within the monomeric TR-PEs on effect specific protein residues through chemical environment alteration. This was followed by increased temperatures in the NMR probe where TR-PEs would have been in the coacervate phase and repeated analysis of chemical environment changes.

The monomer effects on ubiquitin were analyzed with NMR at 5°C. Generally, many ubiquitin-polymer resonances experienced a near uniform CSP that was virtually identical to the reference spectrum collected on free ubiquitin collected at the same

temperature. This was not indicative to polymer directly effecting ubiquitin or binding under polymer soluble conditions. A spectrum comprised of an overlay between a 100 μM reference ^{15}N ubiquitin and the various ubiquitin-polymer samples showed multiple significant CSS events (**Figure 5.1**). At this temperature, the signal from ^{15}N natural abundance within concentrated polymer were observed and labelled. Many of the reference ubiquitin's surface lysine resonances were slightly broadened with a low signal to noise ratio, suggesting chemical exchange. These surface residues likely exist in varying states which decreases individual intensity. After combination with polymer samples, those corresponding resonances sharpened and were visualized. This indicated that K6, K11, K29, and K63 experienced a significant change in chemical environment with polymer present. It was possible that these resonances exhibited slow exchange on the NMR chemical shift timescale within the reference spectrum and the signals were broadened into the noise. It was speculated that polymer addition induced conformational constraints within individual residues but could also be due to subtle changes in the dielectric environment, i.e. "saltiness" of the solution. This influenced how often a given residue existed within a specific state, thus, sharpening the signal. Although these changes are nondiscriminatory between polymer variants, it was confirmed that polymers are nonspecifically interacting with ubiquitin's surface residues.

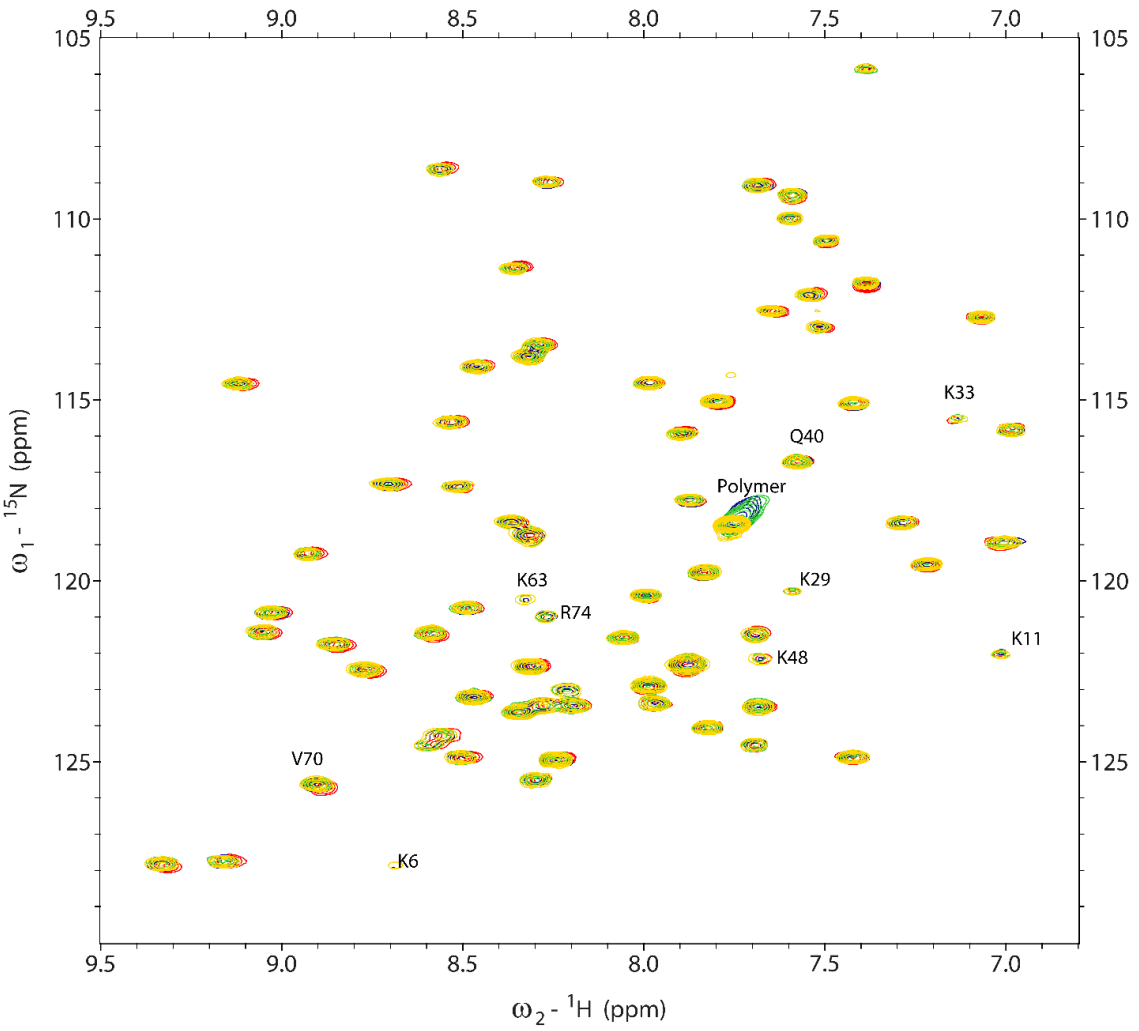

Figure 5.1. Overlay spectrum from ^{1}H – ^{15}N HSQC of all samples at 5°C. Red, ^{15}N ubiquitin. Blue, ubiquitin with polymer 1. Green, ubiquitin with polymer 2. Gold, ubiquitin with polymer 3. Various ubiquitin residues that experienced change in chemical environment were labelled. Signal produced from polymer due to the natural abundance of ^{15}N was visualized within spectra and was labelled 'Polymer'.

Samples were subjected to a 25°C probe temperature which encouraged the formation of coacervate droplets within sample. This explored interactions between ubiquitin and TR-PEs in the coacervate phase. Immediate differences were found within

the reference spectrum as an increased temperature increased the exchange rate on the NMR chemical shift timescale, which provided better-resolved signal (**Figure 5.2**). CSPs occurred at the K6, K33, I44, F45, and H68 resonances and shifted in the ^{1}H, ^{15}N, or both dimensions, visualized on the spectrum. This indicated that these specific residues experienced chemical environment alterations related to binding or association while polymer was within the coacervate phase. It was significant that CSP occurred at the H68 resonance. Histidine contains an imidazole side chain, which is slightly protonated at pH 7.4. Given that this CSP occurs in all polymer samples, it was likely that the imidazole in H68 was interacting with the common polymer unit [EoEtA]. CSB events occurred unanimously within ubiquitin-polymer samples at the L8, T9, K11, L12, K63, L69, R74, and G75 resonances. Intensity loss was theorized to be associated with higher local concentration within droplets or reduction of protein tumbling in presence of coacervate droplets. Polymer signal appeared within spectra at this temperature, however, the resulting signals were different between the polymer variants. No conclusion was drawn concerning the Q40 resonance due to overlap with polymer interference.

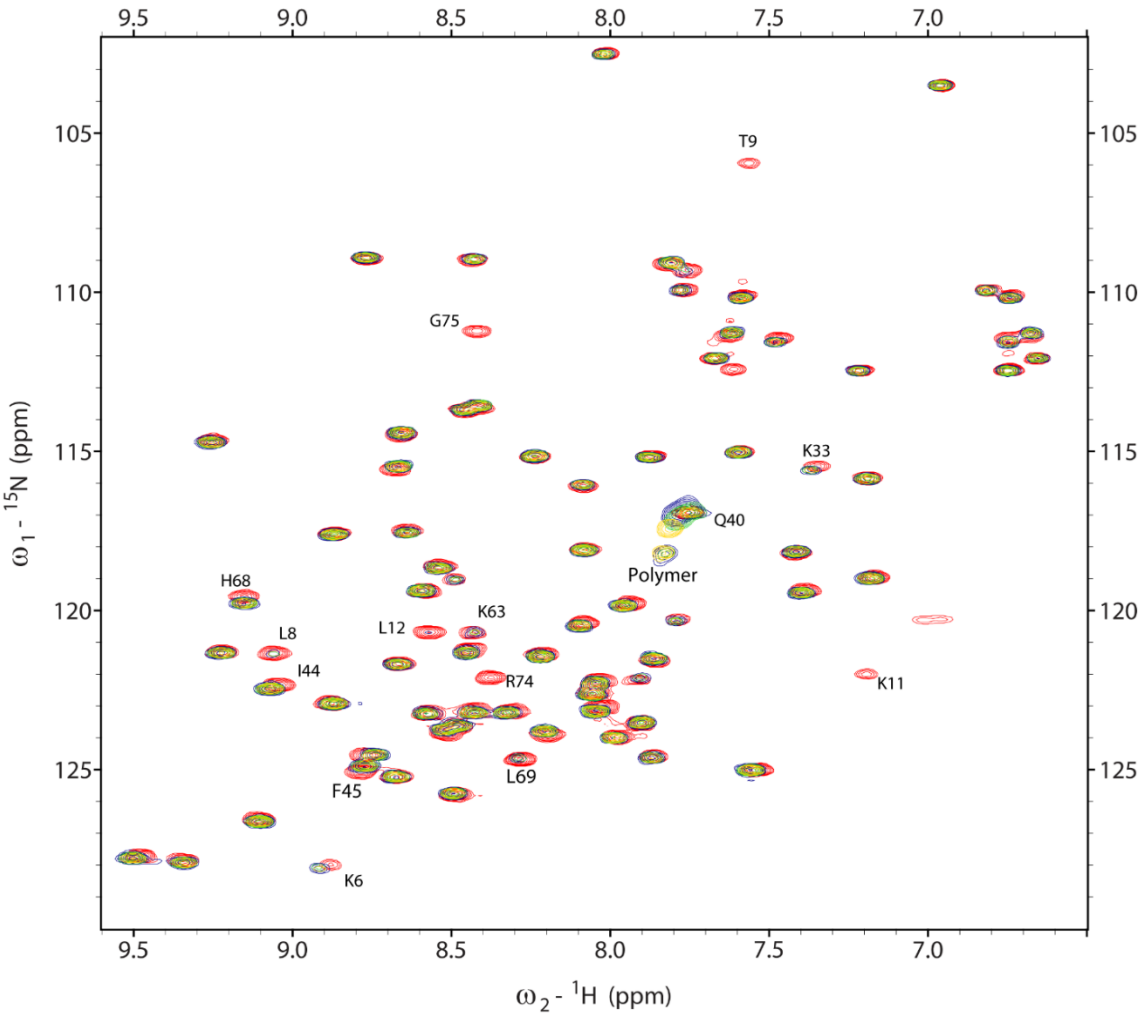

Figure 5.2. Overlay spectrum from ^{1}H - ^{15}N HSQC of all samples at 25°C. Red, ^{15}N ubiquitin. Blue, ubiquitin with polymer 1. Green, ubiquitin with polymer 2. Gold, ubiquitin with polymer 3. Various ubiquitin residues that experienced chemical shift changes were labelled. Signal produced from polymer due to the natural abundance of ^{15}N was visualized within spectra and was labelled 'Polymer'.

At temperature conditions where a typical protein might degrade, the reference ubiquitin proved that protein structure was retained for this temperature. Samples introduced to higher temperature, 45°C, ensured that TR-PEs existed in the coacervate phase and provided sharper signals for the fingerprinting analysis (**Figure 5.3**). CSBs

were observed across polymer variants with resonances for K6, K11, T14, K33, D39, Q49, and G76. This was similar to experiments at 25°C. All polymer variants induced a CSP at the Q2 resonance, which suggested that the common polymer unit [EoEtA] influenced this change in chemical environment. Polymer variants 2 and 3, with the unique pendant groups [mTrp] and [mAla] respectively, permitted significantly different CSPs at resonances K48, N60, and K63 when compared to polymer 1 [mPhe], which did not exhibit any CSP. This was an interesting occurrence, as it was originally expected that polymers 1 and 2 would cause CSP within sample.

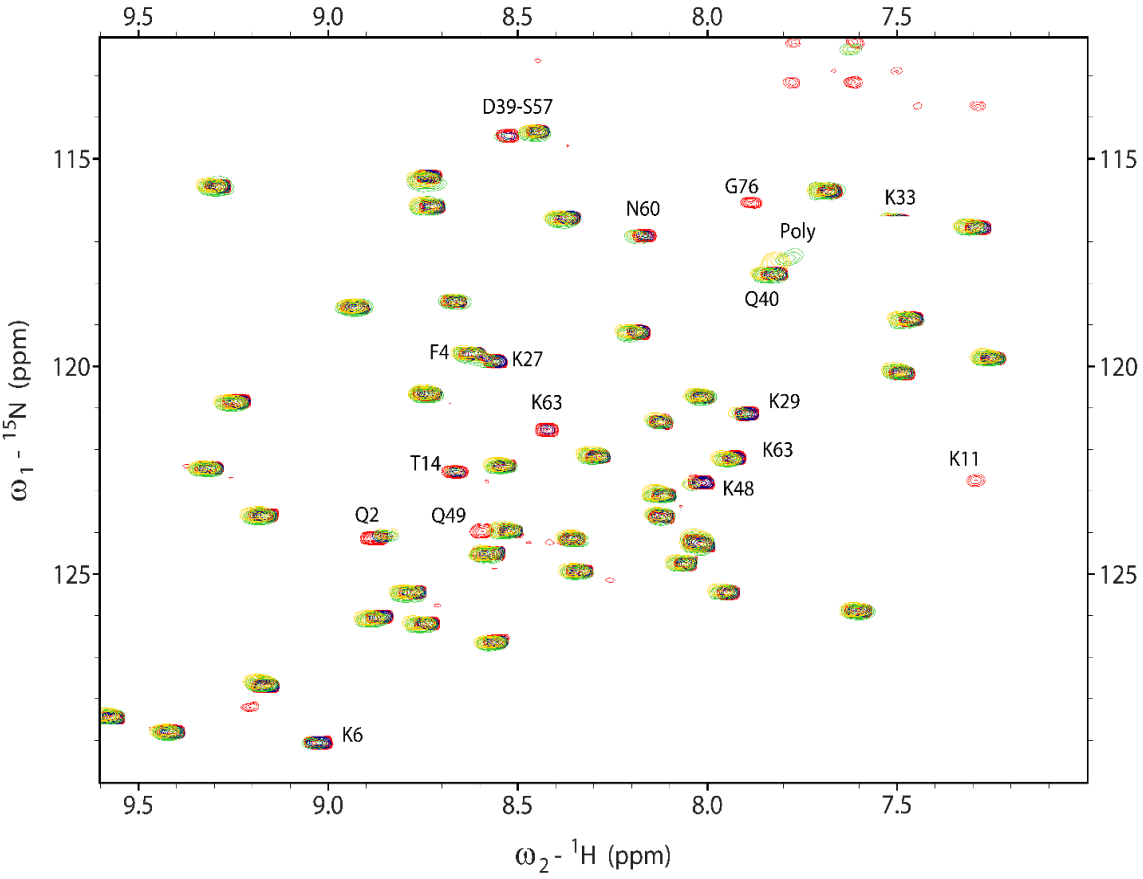

Figure 5.3. Overlay spectrum from ^{1}H - ^{15}N HSQC of all samples at 45°C. Red, ^{15}N ubiquitin. Blue, ubiquitin with polymer 1. Green, ubiquitin with polymer 2. Gold,

ubiquitin with polymer 3. Various ubiquitin residues that experienced chemical shift changes were labelled.

When comparing the negative control spectrum (**Appendix 4.3**) to the sample overlay spectrum (**Figure 5.3**), it was observed that signal surrounding resonance Q40 has no corresponding signal within the control. This suggested that polymers 2 and 3 were interacting with this glutamine residue and caused the signal splitting. Glutamine contains carboxylic acid and amide functional groups within its side chain. Furthermore, Q40 is a surface exposed residue on ubiquitin and is more reasonable to be interacting with the TR-PEs, which suggests that polymers 2 and 3 provide improved encapsulation of ubiquitin.

Pooling information from fingerprint analysis of the three highlighted VT-NMR series confirmed that TR-PEs interacted with ubiquitin and its overall structure was retained. It was concluded that minimal specific association occurred between ubiquitin and TR-PEs within the aqueous phase, 5°C; this was signified by CSS of surface lysine residues and absence of CSP events. More significant interactions occurred within samples where TR-PEs were within the coacervate phase. This was interpreted that the coacervate droplet environment encourages more specific surface interfacing with ubiquitin's specific residues like K6, K33, and H68 at 25°C and Q2, Q40, and N60 at 45°C. Overall, ubiquitin structure was preserved and TR-PEs main effects on ubiquitin remain in nonspecific associations, however, the individual CSP events hint at the less common specific interactions.

Chapter Six

CONCLUSIONS, FUTURE WORK, AND IMPACT

Conclusions

TR-PEs have potential for future use as small molecule packaging systems. The polymers used within this work have intrinsic biodegradability, under acidic conditions, and possible activity with esterases. They break down into non-harmful byproducts that can be eliminated from a biological system, giving way to potential use as a therapeutic packaging system. A greater understanding of this capability required the use of model protein cargos.

These model protein cargos were produced to create an efficient and reliable source of sample to a degree acceptable for application. Although the ubiquitin IEC purification remained tedious, requiring multiple SDS-PAGE analysis between purification steps, pure ubiquitin sample was obtained. The purification method was customized to produce ^{15}N isotopically labeled ubiquitin for use with VT-NMR. In contrast, the β-gal IMAC purification was robust and provided pure β-gal for use in colorimetric kinetic assays and fluorescence-based analysis.

Specific activity and R_n calculations pertaining to β-gal that had experienced the encapsulation process were integral to determining the effects of TR-PE encapsulation on the protein's integrity. The SA and R_n, values normalized against protein concentration,

enabled comparison between the various samples collected through the encapsulation protocol. Direct comparison between the harvest sample, H, and the fourth supernatant sample, S4, was permitted due to being of equal dilution. If protein was not retained in the coacervate droplets, then the SA comparisons would be equal in value. If protein was negatively impacted through TR-PE encapsulation, then sample H SA would be a lesser value than sample S4. In contrast, β-gal that was encapsulated and retained activity within sample H would likely display SA and R_n values greater than the sample S4. This analysis was used to elucidate the varying effects of TR-PEs on β-gal enzymatic activities.

Polymers 1, 3, 5, and 6 were demonstrated to effectively capture and preserve β-gal activity. Whereas polymers 2, 4, and 7 were able to effectively capture β-gal but did not preserve its activity as well. Each polymer sample contained different retention rates for recovered protein. These data suggested that inherent characteristics among TR-PEs were modified with varying pendant group monomer units. Which contributes to the attraction of exploring the use of these modular pendant groups within polymers to influence the environment where protein was encapsulated.

Building on the encapsulation data with CFM, TR-PE samples 1-7 were shown to capture and isolate FITC-β-gal through the encapsulation process. It was suspected that aggregated FITC-β-gal was visualized within droplets, confirming the presence of negatively impacted protein, which was corroborated by the SA and R_n analyses. It was also indicated, by fluorescent localization of FITC-β-gal, that different polymers form different average coacervate droplet sizes. This suggested that the pendent groups

influence the physical droplet characteristics and could possibly be optimized to encapsulate target model protein cargos at higher retention rates.

Biophysical analysis of TR-PE effects on the model ubiquitin cargo utilizing VT-NMR demonstrated that ^{15}N-ubiquitin's structure was preserved throughout interactions with polymer samples 1, 2, 3, and 5. When TR-PEs were monomeric within the aqueous phase, 5°C, interactions with ^{15}N-ubiquitin were focused on polar surface residues such as lysine. The CSS events at residues K6 and K63 indicate that tested monomers altered the chemical environment of these surface lysine residues. This likely encouraged these residues to exist more often within a certain conformation, which increases a resonance's T2 and thus intensity of its related peak. These effects were observed for all tested polymer samples, which contained varying pendant groups, and were likely caused by the polymer backbone.

As coacervate droplets were formed at 25°C, significant CSP events occurred within all tested polymers at specific residues K6, K33, and H68. Other resonances produced within the ubiquitin-polymer samples experienced CSB. It remained inconclusive as to why the previous resonances were perturbed; experimentation at 45°C did not display similar CSP when compared to 25°C. Significant CSP occurred within all tested polymers at residues Q2 and Q40. CSP for Q2 was uniform, but the CSPs at residue Q40 varied between polymers. CSP unique to polymers 2 and 3 occurred at N60. It was originally theorized that polymers 1 and 2 would cause significant CSP. That was not the case. Polymers 2 and 3 have the pendant groups [mTrp] and [mAla] respectively. It was interesting to note that polymer 3 would result in N60 perturbation, as it was a polar surface residue.

In summary, these VT-NMR data hint that nonspecific interactions occurred between ubiquitin and polymer when they were monomers within solution. Many of the CSB events were displayed with all tested polymers. It was possible that the pendant group frequency within the copolymer was too low to create a significant impact. With a better understanding of ubiquitin-polymer interactions, inferences were made that TR-PEs will similarly impact β-gal. Mainly surface residues were interacted with within solution, but there was possibility for TR-PEs to interact with specific residue sites on β-gal; this might have been beneficial or detrimental, as polymer 2 contained a high retention rate but was shown to negatively affect β-gal specific activity. A comparison between these two model-proteins was difficult to establish because of their differences in function and their molecular sizes.

This work described the potential of TR-PEs as a potential small molecule packaging system by studying the effects on model proteins through both bioanalytical and biophysical methods. These coacervate forming biodegradable TR-PEs demonstrated the capability to encapsulate and release a model protein while preserving its integrity - polymers 1, 3, 5, and 6. Additional time and research would allow the further development and optimization of these polymers into a future potential therapeutic packaging system.

Future Work

Further development of purification protocols for ^{15}N-ubiquitin would be beneficial in the long run. Investigating more efficient protein preparations would not

only reduce long term cost of reagents, like ^{15}N ammonium chloride, it would allow researchers to spend less time with protein preparations and more time on experimentation and analysis. The purification process was the most prominent bottleneck to improve upon. SDS-PAGE analysis was required at each purification step, which increased the time delay before proceeding with the next step. The gradient elution step within the CEC purification should be optimized to better resolve ubiquitin's elution from other proteins. This should be done by modulating the salt concentration and column flow rates. After optimization, ubiquitin yields (mg/L) should increase.

Furthering the use of CFM for encapsulation characterization could benefit interpretations from fluorescence microscopy. Higher magnification droplet analysis using oil immersion techniques would increase resolution of captured proteins and produce higher quality images. Kennesaw State University's confocal microscope has four different fluorescence channels and could be modulated to study fluorescently labeled polymer tandem with a FITC-labeled protein. This would produce beneficial information on polymer structure in relation to the FITC-labeled protein. CFM pilot assays were conducted with FITC-ubiquitin but were not included in this work. Further optimization of labeling protocols and CFM conditions are required to improve experimental value. When analyzing droplet sizes, flow cytometry would be useful to determine the TR-PEs physical droplet sizes more accurately.

Ubiquitin was used for biophysical analysis of interactions with TR-PEs. Various NMR analysis techniques could be applied to improve the understanding of how ubiquitin was affected by TR-PEs. Line-shape analysis of previously obtained ^{1}H-^{15}N HSQC spectra, from VT-NMR, could provide insight into exchange dynamics assumed

to occur within the ubiquitin-polymer samples. Exploring a different mode of experimentation where ubiquitin is processed through the encapsulation and wash sequence to purely study ubiquitin within the droplet environment could influence the interpretations on whether modulating the pendant groups within the copolymer is beneficial for increased encapsulation. Finally, STD NMR, which focuses analysis on hydrogens within the copolymer, could be revisited to examine if certain hydrogen atoms experience chemical environment alterations in the presence of ubiquitin.

Utilizing ubiquitin within encapsulation studies, like those conducted with β-gal, would broaden the model protein cargo's scope within future projects. After applying the encapsulation and wash process to ubiquitin, samples could be quantitated with SDS-PAGE analysis or UV-VIS (A_{280}) to compare the various protein retention rates between polymer variants. Combining this assay type with data from the previously obtained VT-NMR spectra might provide further evidence if the pendant groups effect protein encapsulation.

A novel experiment could include the use of ubiquitin conjugating enzymes. The encapsulation and wash process would be conducted to isolate ubiquitin within droplets. Then after encouraging the release of ubiquitin, a researcher would add E2 ubiquitin-conjugating enzyme along with ATP. SDS-PAGE analysis would demonstrate if ubiquitin ladders were formed. This would aid in determining whether ubiquitin retains its functional purpose as a substrate after interaction with various TR-PEs.

Impact

The unique work contained within this thesis document provides insight to the effects of the coacervate forming biodegradable TR-PEs on the model protein cargos, β-gal and ubiquitin. Although nanogel systems have shown β-gal capture, β-gal has not been previously shown to be efficiently captured within coacervate forming biodegradable TR-PEs. This work is important in demonstrating that, with more time and research, TR-PEs hold potential for a protein packaging system that can preserve the integrity of its targeted cargo.

REFERENCES

1. Zhang, Z.; Gao, F.; Jiang, S.; Ma, L.; Li, Y., Nano-based Drug Delivery System Enhances the Oral Absorption of Lipophilic Drugs with Extensive Presystemic Metabolism. *Current Drug Metabolism* **2012,** *13* (8), 1110-1118.

2. Dimitrov, D. S., Therapeutic Proteins. Humana Press: 2012; pp 1-26.

3. Goeddel, D. V.; Kleid, D. G.; Bolivar, F.; Heyneker, H. L.; Yansura, D. G.; Crea, R.; Hirose, T.; Kraszewski, A.; Itakura, K.; Riggs, A. D., Expression in Escherichia coli of chemically synthesized genes for human insulin. *Proc Natl Acad Sci U S A* **1979,** *76* (1), 106-110.

4. Egrie, J. C.; Browne, J. K., Development and characterization of novel erythropoiesis stimulating protein (NESP). *British Journal of Cancer* **2001,** *84* (1), 3-10.

5. Crommelin, D.; Bermejo, T.; Bissig, M.; Damiaans, J.; Krämer, I.; Rambourg, P., Pharmaceutical evaluation of biosimilars: important differences from generic low-molecular-weight pharmaceuticals. *Eur J Hosp Pharm Sci* **2005,** *11* (1), 11-7.

6. Kessler, M.; Goldsmith, D.; Schellekens, H., Immunogenicity of biopharmaceuticals. *Nephrology Dialysis Transplantation* **2006,** *21* (suppl_5), v9-v12.

7. Kousalová, J.; Etrych, T., Polymeric nanogels as drug delivery systems. *Physiological research* **2018,** *67 Supplementum 2*, S305-S317.

8. Soni, K. S.; Desale, S. S.; Bronich, T. K., Nanogels: An overview of properties, biomedical applications and obstacles to clinical translation. *Journal of Controlled Release* **2016,** *240*, 109-126.

9. Bhuchar, N.; Sunasee, R.; Ishihara, K.; Thundat, T.; Narain, R., Degradable thermoresponsive nanogels for protein encapsulation and controlled release. *Bioconjug Chem* **2012,** *23* (1), 75-83.

10. Cruz, M. A.; Morris, D. L.; Swanson, J. P.; Kundu, M.; Mankoci, S. G.; Leeper, T. C.; Joy, A., Efficient Protein Encapsulation within Thermoresponsive Coacervate-Forming Biodegradable Polyesters. *ACS Macro Letters* **2018,** *7* (4), 477-481.

11. Anderson, E. H., Growth Requirements of Virus-Resistant Mutants of Escherichia Coli Strain "B". *Proc Natl Acad Sci U S A* **1946,** *32* (5), 120-128.

12. Ma, D.; Shen, L.; Wu, K.; Diehnelt, C. W.; Green, A. A., Low-cost detection of norovirus using paper-based cell-free systems and synbody-based viral enrichment. *Synthetic Biology* **2018,** *3* (1).

13. Hajebi, S.; Rabiee, N.; Bagherzadeh, M.; Ahmadi, S.; Rabiee, M.; Roghani-Mamaqani, H.; Tahriri, M.; Tayebi, L.; Hamblin, M. R., Stimulus-responsive polymeric nanogels as smart drug delivery systems. *Acta Biomater* **2019,** *92*, 1-18.

14. Swanson, J. P.; Monteleone, L. R.; Haso, F.; Costanzo, P. J.; Liu, T.; Joy, A., A Library of Thermoresponsive, Coacervate-Forming Biodegradable Polyesters. *Macromolecules* **2015,** *48* (12), 3834-3842.

15. Nair, L. S.; Laurencin, C. T., Polymers as Biomaterials for Tissue Engineering and Controlled Drug Delivery. In *Tissue Engineering I*, Lee, K.; Kaplan, D., Eds. Springer Berlin Heidelberg: Berlin, Heidelberg, 2006; pp 47-90.

16. Michaelis, L.; Menten, M. L., Die kinetik der invertinwirkung. *Biochem. z* **1913,** *49* (333-369), 352.

17. Briggs, G. E.; Haldane, J. B. S., A note on the kinetics of enzyme action. *Biochemical journal* **1925,** *19* (2), 338.

18. Bradford, M. M., A rapid and sensitive method for the quantitation of microgram quantities of protein utilizing the principle of protein-dye binding. *Analytical Biochemistry* **1976,** *72* (1), 248-254.

19. Maeda, H.; Ishida, N.; Kawauchi, H.; Tuzimura, K., Reaction of fluorescein-isothiocyanate with proteins and amino acids I. Covalent and non-covalent binding of fluorescein-isothiocyanate and fluorescein to proteins. *The Journal of Biochemistry* **1969,** *65* (5), 777-783.

20. Riggs, J.; Seiwald, R.; Burckhalter, J.; Downs, C. M.; Metcalf, T., Isothiocyanate compounds as fluorescent labeling agents for immune serum. *The American journal of pathology* **1958,** *34* (6), 1081.

21. Sarkar, S. K.; Bax, A., A simple and sensitive one-dimensional NMR technique for correlation of proton and carbon chemical shifts. *Journal of Magnetic Resonance (1969)* **1985,** *62* (1), 109-112.

22. Fesik, S. W.; Eaton, H. L.; Olejniczak, E. T.; Zuiderweg, E. R.; McIntosh, L. P.; Dahlquist, F. W., 2D and 3D NMR spectroscopy employing carbon-13/carbon-13 magnetization transfer by isotropic mixing. Spin system identification in large proteins. *Journal of the American Chemical Society* **1990,** *112* (2), 886-888.

23. Kundu, M.; Morris, D. L.; Cruz, M. A.; Miyoshi, T.; Leeper, T. C.; Joy, A., Elucidating the Molecular Interactions of Encapsulated Doxorubicin within a Nonionic, Thermoresponsive Polyester Coacervate. *ACS Applied Bio Materials* **2020,** *3* (7), 4626-4634.

APPENDIX ONE

1.1 Recipes for buffers used in β-gal expression and purification

Buffer Name	Running Buffer "Buffer A"	Elution Buffer "Buffer B"	SEC/Dialysis Buffer
Volume	1 Liter	1 Liter	1 Liter
pH adjustment	8.0	8.0	8.0
Dibasic Potassium Phosphate K_2HPO_4 (Anhydrous)	20 mM 3.846 g	20 mM 3.846 g	20 mM 3.846 g
Monobasic Potassium Phosphate KH_2PO_4 (Anhydrous)	20 mM 2.722 g	20 mM 2.722 g	20 mM 2.722 g
Potassium Chloride KCl	200 mM 14.910 g	200 mM 14.910 g	200 mM 14.910 g
Imidazole	20 mM 1.362 g	400 mM 27.232 g	———
Sterilization	0.22 µM Filter	0.22 µM Filter	0.22 µM Filter

1.2 Recipes for buffers used in ubiquitin expression and purification

Buffer Name	Running Buffer "Buffer C"	Elution Buffer "Buffer D"	SEC/Dialysis Buffer "1x PBS"
Volume	1 Liter	1 Liter	1 Liter
pH adjustment	5.0	5.0	7.4
Sodium Acetate $NaCH_3COO$	50 mM 6.804 g	50 mM 6.804 g	———
Disodium EDTA	5 mM 1.8611 g	5 mM 1.8611 g	———
Sodium Chloride NaCl	———	1 M 58.44 g	137 mM 8.0 g
Dibasic Potassium Phosphate K_2HPO_4 (Anhydrous)	———	———	1.8 mM 0.24 g
Disodium Phosphate Na_2HPO_4 (Anhydrous)	———	———	10 mM 1.44 g
Potassium Chloride KCl	———	———	2.7 mM 0.20g
Sterilization	0.22 µM Filter	0.22 µM Filter	Filter or Autoclave

APPENDIX TWO

2.1 SOP for Beta-Galactosidase Encapsulation Kinetics Assay with Polymer Reconstitution

Total experimental time: 140-245 minutes

I. Principle of Concept

Efficient encapsulation and release of the β-gal model protein with thermoresponsive coacervate-forming biodegradable polyesters TR-PEs provides the foundation for their potential use as therapeutic delivery systems. These kinetics assays compare capture efficiency and enzyme activity preservation between polymer samples. Polymers thought to be favorable for capturing high molecular weight biomolecules are screened and evaluated for future research application. The following figure briefly describes the encapsulation process.

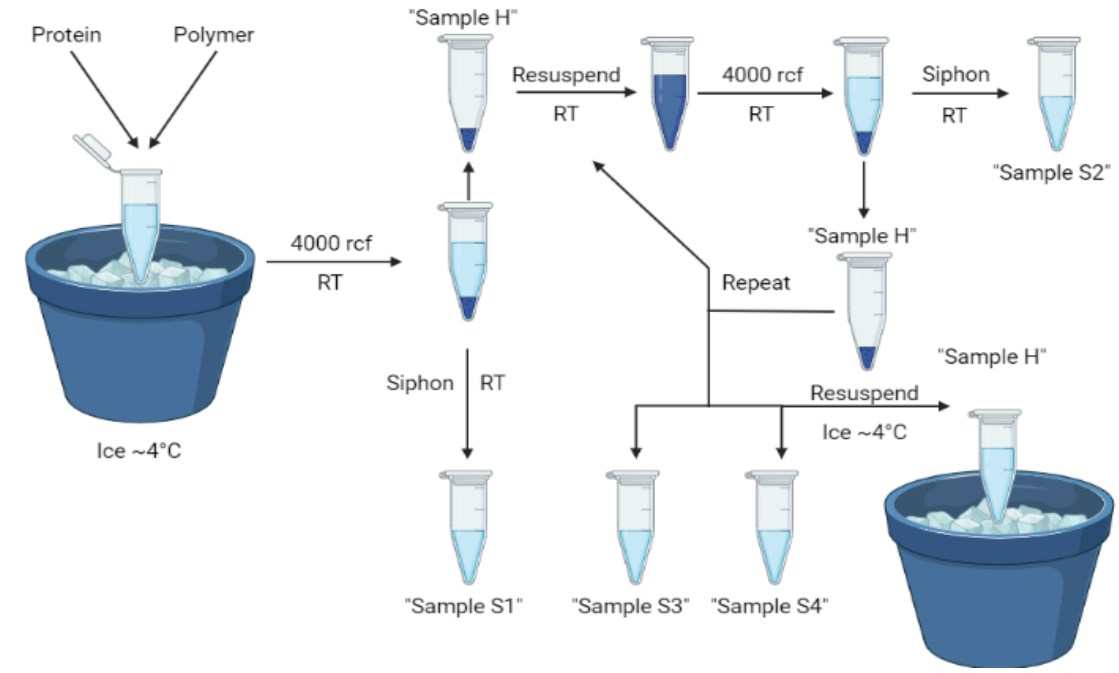

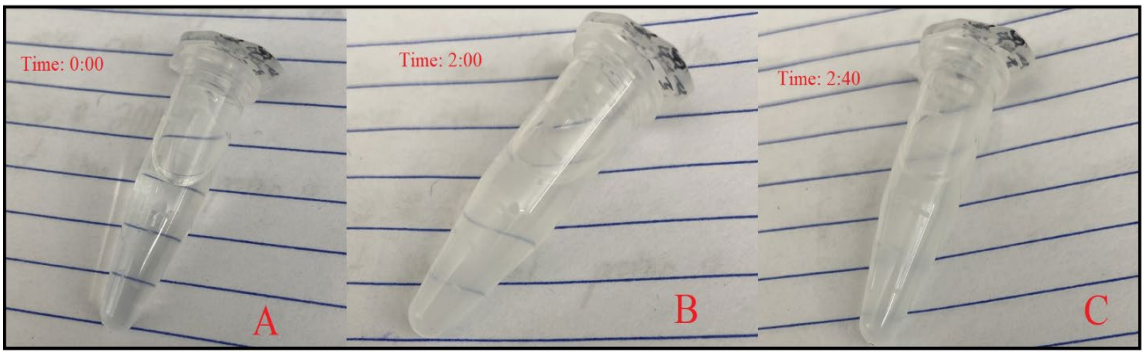

Images showcased the coacervation of any given polymer after reconstitution. Panel A showed the monomers within solution indicated by its transparency after immediately removed from ice. Panel B showed the coacervate droplets forming two minutes after removal from ice. Panel C showed the full coacervation of the polymer mixture at two minutes and forty seconds after removal from ice. Coacervation is indicated by the increase of optical density.

II. **Resources**

Material/Reagents	Source	CAS/Catalog No.	Amount Needed
Polymer	Joy Laboratory	--	20 mg/mL—100uL/Assay
1.7mL Eppendorf tubes	Genesee Scientific	Cat #: 22-281	5 per/Assay--As needed
96-Well Plate, black, clear bottom	Corning: Life Sciences	Cat #: 3631	1
Beta-Galactosidase	In-house purification	--	20µM—100uL/Assay
CPRG	Sigma Aldrich	CAS: 99792-79-7 Cat #: 10884308001	1mM—200uL/Assay
1x PBS pH: 7.4	Lab Stock	--	As needed
Ice	Ice machine	--	Bucket of Ice

III. **Polymer Reconstitution Protocol**

a. Preparation (Time required: 10-30 minutes)

i. Obtain the desired solid polymer located within freezer. Weigh the designated amount of polymer into a 1.7 mL Eppendorf (epi) tube on a weigh boat. The polymer can be cut with a razor or X-Acto-

knife on a separate weigh boat to then load into the tube. It is **important** to do this while still polymer is still frozen. If thawed, the polymer will be gooey and more difficult to weigh and obtain an accurate amount.

ii. Add PBS buffer to the epi tube with polymer and close the tube. Amount of buffer should result with a polymer concentration of 20 ± 1 mg/mL. Specifically note the concentration.

iii. Label the tube with polymer number, concentration, initials, and date. May also use label tape specifically used for NMR tubes and then wrap with parafilm around the side of the tube to ensure labelling is not removed by subsequent steps.

b. **Reconstitution (30-60 minutes)**

i. Vortex for approximately 30 seconds; do this until the mixture becomes cloudy. Place the tube in ice for about 1 or 2 minutes; leave the tube on ice until the mixture/solution becomes clear. Repeat the vortex and chilling steps until the polymer is completely reconstituted into solution.

ii. When finished, check the label's integrity, and then store in -20°C.

1. **Note:** freeze thaw cycles may encourage more efficient reconstitution. May be beneficial to repeat the vortex and chill process.

IV. **Beta-Galactosidase Encapsulation Kinetics Assay Protocol**

a. **Preparation (10-20 minutes)**

i. Beta-galactosidase at approximately 20 μM. Stock protein is kept in the -80°C. Aliquots of 20 μM protein should be made for individual experiments, avoid excess freeze-thaw cycles. If protein is not available, it should be made in-house using standard protein expression and IMAC purification protocols.

ii. Polymer stock at 20 mg/mL. Refer to "Polymer Reconstitution Protocol" if polymer is not available.

iii. When creating samples, 5 epi tubes will be needed per experiment. Label one with 'H' (for the harvest step), 'S1' 'S2' 'S3' 'S4' (for the subsequent supernatant wash steps).

iv. CPRG in 1mM aliquots. If not available, CPRG reagent is in the -20°C. Make 10 mLs of 10 mM CPRG stock. 60.74 mg CPRG, 10 mLs of filtered 18MOhm water. Freeze (-20°C) in 1 mL aliquots or dilute into 1 mM aliquots for colorimetric assay.

b. **Sample creation (30-60 minutes)**

i. On ice, add 100uL of β-gal , then add 100uL of polymer to the 'H' epi tube. While on ice, polymers should remain in the aqueous phase. Pull aliquots of 1mM CPRG for the kinetic assay to thaw on the bench/tube rack. **Reminder:** 200uL needed for each well reaction; be sure to pull the amount needed ahead of time.

ii. Remove the 'H' epi from ice and place it into a tube rack. When warming up to room temperature, the polymer should begin to coacervate and capture protein. Return to ice once fully in the

coacervate phase. Again, once the polymer is completely in aqueous phase, return to the tube rack. This will be ready for the centrifugation and wash steps.

iii. Put the harvest sample and balance into the Eppendorf *Centrifuge 5418* table top centrifuge with the FA-45-18-11 rotor. Spin at 3000-5000 rcf (dependent on the polymer's molecular weight) for 1.5 minutes. This is done to obtain a pellet of coacervated polymer with captured protein. Remove the tube and keep it in its orientation from the centrifuge to keep the pellet intact. If the supernatant is still cloudy, increase the rcf and spin again.

iv. Once a pellet is obtained with a clear supernatant, carefully siphon off the supernatant using a p100 micropipette. Eject supernatant into the 'S1' tube. Remove as much supernatant as possible without altering the integrity of the coacervate pellet. All 'S#' tubes can remain in the tube rack.

v. Add 200uL of 1x PBS pH 7.4 buffer in 100uL increments. Eject the buffer in a fashion to directly impact the pellet. Then tap the tube to disturb the pellet and distribute coacervate droplets throughout the buffer mixture. At room temperature the droplets will not return to the aqueous phase. Captured protein should remain captured. Any protein caught interstitial to the droplets will be diluted into the buffer. The idea is that washing the coacervates

will provide an accurate activity measurement of captured protein when released.

vi. Repeat steps “iii – v” to fill the ‘S2, 3, 4’ tubes with the corresponding supernatant wash steps.

vii. After the wash steps, add the final 200uL of buffer to the harvest sample. Tap the tube to disturb the final pellet. Then place the tube on ice. This will encourage the coacervate droplets to return to the aqueous phase and release the captured protein.

c. **Colorimetric Assay (i-iii 15-30 minutes) (iv 45 minutes) (v ∞)**

i. **Planning** the kinetic assay and layout of the 96-well microplate. Following is an example plate of sample and standard placement. Row A is a standard concentration series from a previous experiment. A standard series should be used to compare the encapsulation experiments relative to a known protein concentration. Row B is a standard repetition layout of two samples. It is best to alternate the samples and have similar samples adjacent to allow simpler pipetting.

	1	**2**	**3**	**4**	**5**	**6**	**7**	**8**	**9**	**10**	**11**	**12**
A	23µM	2.8µM	1.84µM	920nM	460nM	230nM	92nM	46nM	23nM	11.5nM	9.2nM	Buffer
B	A H	B H	AS1	BS1	AS2	BS2	AS3	BS3	AS4	BS4	23µM	Buffer

ii. **Reagent and sample preparation**. Aliquots of 1mM CPRG should have been pulled in 'Step B1', if not, pull and thaw now. A source of 1x PBS pH 7.4 buffer is needed. Obtain a black, clear bottom 96-well microplate. The harvest samples (tubes labeled with 'H') and any protein samples need to remain on ice. The supernatant wash samples may remain in a tube rack at room temperature. Organize the samples to reflect the plate organization previously planned. Gloves, p10 and p1000 micropipettes, and a tip waste container will also be needed.

iii. **Plate reader parameters.** Kinetic assay. One point absorbance: 574nm. Temperature: 22C. Read area: Select all wells that will be analyzed. Read timing: 30-minute experiment, 20 second read intervals. Shake: 3 second medium orbital. Plate layout: designate harvest samples, supernatant wash samples, standard, and buffer in their respective wells. Example images in appendix.

iv. **Experimental procedure.** Using a p1000, pipette 200uL 1mM CPRG into each experimental well. Eject CPRG along the inner edge of the well to negate any bubbles. Using a p10, pipette 10uL of each sample into their corresponding well in the following order: Buffer, S4, S3, S2, H, S1, and Standard β-gal. Put the microplate into the plate-reader, close the tray, then start the data collection. This is the most efficient way to initiate the kinetic experiment.

v. **Data analysis.** Upon completion of the experiment, right-click the plate image and click ‘copy plate data’. Paste this data into a shared google spreadsheet on the Ribonauts account. Use this file for data compilation and organization. It is beneficial to provide a brief description of the experiment details for reference; put this above the data. Use GraphPad to conduct further data analysis and evaluation. This will consist of creating figures to best represent and describe the data.

2.2 Bradford standard curve created with purified β-gal

Purified β-gal was used to form a standard curve. Three replicates of known concentrations were tested with Bradford reagent. The error bars are not visible due to replicate tightness. The LOD was calculated to be 27.2 μg/mL.

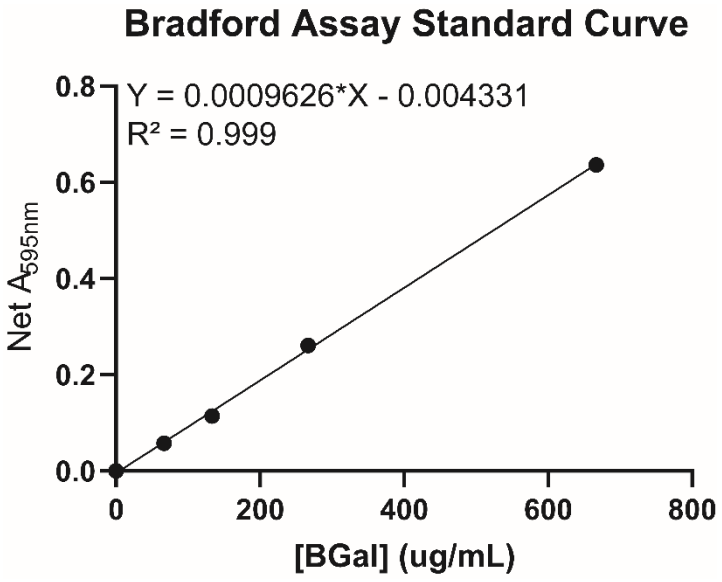

$$\mathbf{LOD} = \mathbf{3.3} * \left(\frac{\boldsymbol{\sigma}}{\mathbf{m}}\right) = \mathbf{3.3} * \left(\frac{\mathbf{0.007934}}{\mathbf{0.0009626}}\right) = \mathbf{27.2}\ \frac{\boldsymbol{\mu}\mathbf{g}}{\mathbf{mL}}$$

2.3 Sample recovery and retention rate calculations

Assayed Polymer Variant	β-gal Recovered (%)	β-gal Retained (%)
P1 (EoEtA-mPhe)	73.4	14.1
P2 (EoEtA-mTrp)	87.9	30.3
P3 (EoEtA-mAla)	61.5	10.8
P4 (EoEtA-mVal)	74.2	18.3
P5 (EoEtA-mTrp-cPrA)	96.8	7
P6 (EoEtA-mPhe-cPrA)	87.1	19.7
P7 (EoEtA-cHex)	95.1	21.7

Delineation between β-gal % Recovered and the % Retained. Both vary throughout each set of assays. Calculations were based on averages calculated from the standard curve read at A_{595}.

Total β-gal Recovered (mg)	0.23
β-gal Loaded (mg)	0.27
% Recovery	87.9

Recovery of β-gal encapsulated with polymer 2. % Recovery was calculated by dividing the total amount of β-gal recovered and measured in the Bradford assay by the initial amount of β-gal combined with TR-PEs.

β-gal in Sample H (mg)	0.07
Total β-gal Recovered (mg)	0.23
% Retention	30.3

Retention of β-gal encapsulated with polymer 2. % Retention was calculated by dividing the amount of β-gal in sample H by the total amount of β-gal recovered.

2.4 Polymer 7 encapsulation kinetics and Bradford figures

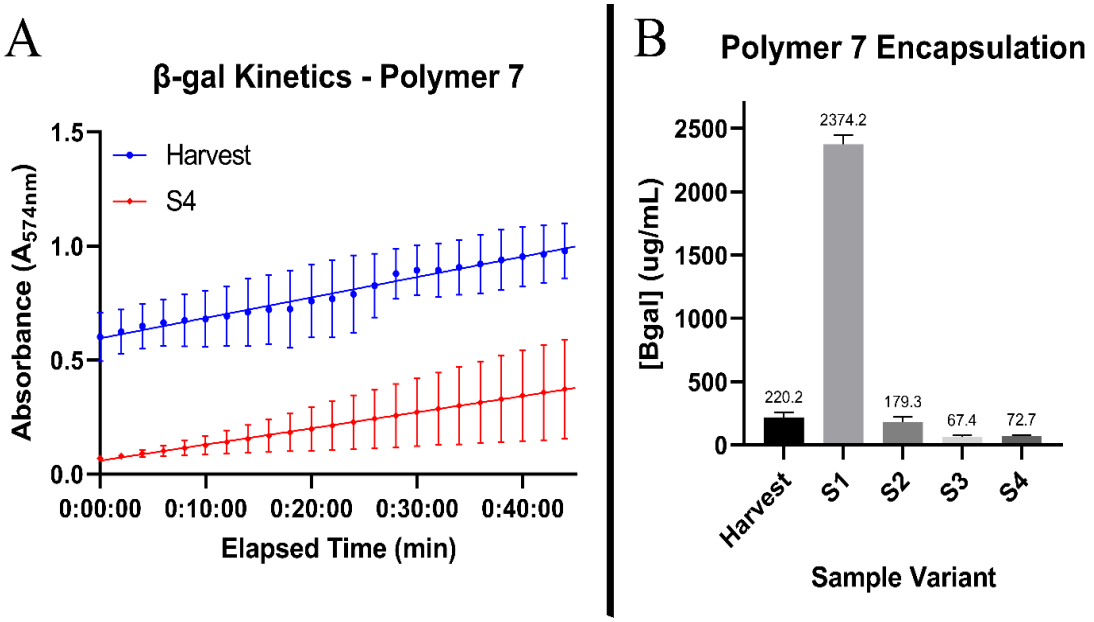

(**A**) β-gal (23 µM) enzymatic assay after encapsulation with polymers 7 (20 mg/mL). The generation of CPR product from CPRG substrate (1 mM) observed at A_{574nm} through 45 minutes at RT. (**B**) Total protein concentration quantitation assay corresponding to various β-gal encapsulation samples. After 30-minute incubation with Bradford reagent at RT, samples were analyzed with an endpoint read at 595 nm.

APPENDIX THREE

3.1 Polymer 7 2D CFM image

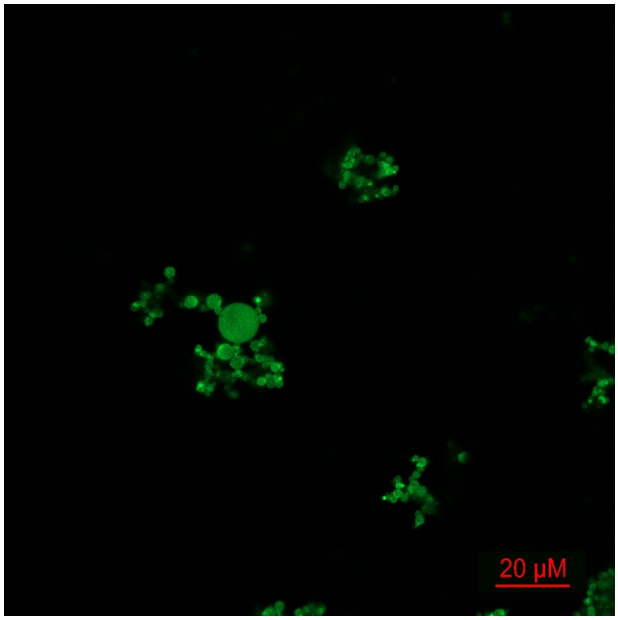

Two-dimensional CFM image (40x magnification, FITC filter) of FITC-β-gal (17.8 µM in 1x PBS pH 7.4) and encapsulated in polymer 7 (EoEtA-cHex) (20 mg/mL in 1x PBS pH 7.4).

APPENDIX FOUR

4.1 Specific pulse program used for experiments

Pulse program: b_trosyetf3gpsi.2; BEST allows better visualization of resonances near water signal. TROSY version of HSQC allows improved resolution and sensitivity for proteins.

4.2 Positive control, VT-NMR Reference ^{15}N-ubiquitin spectra

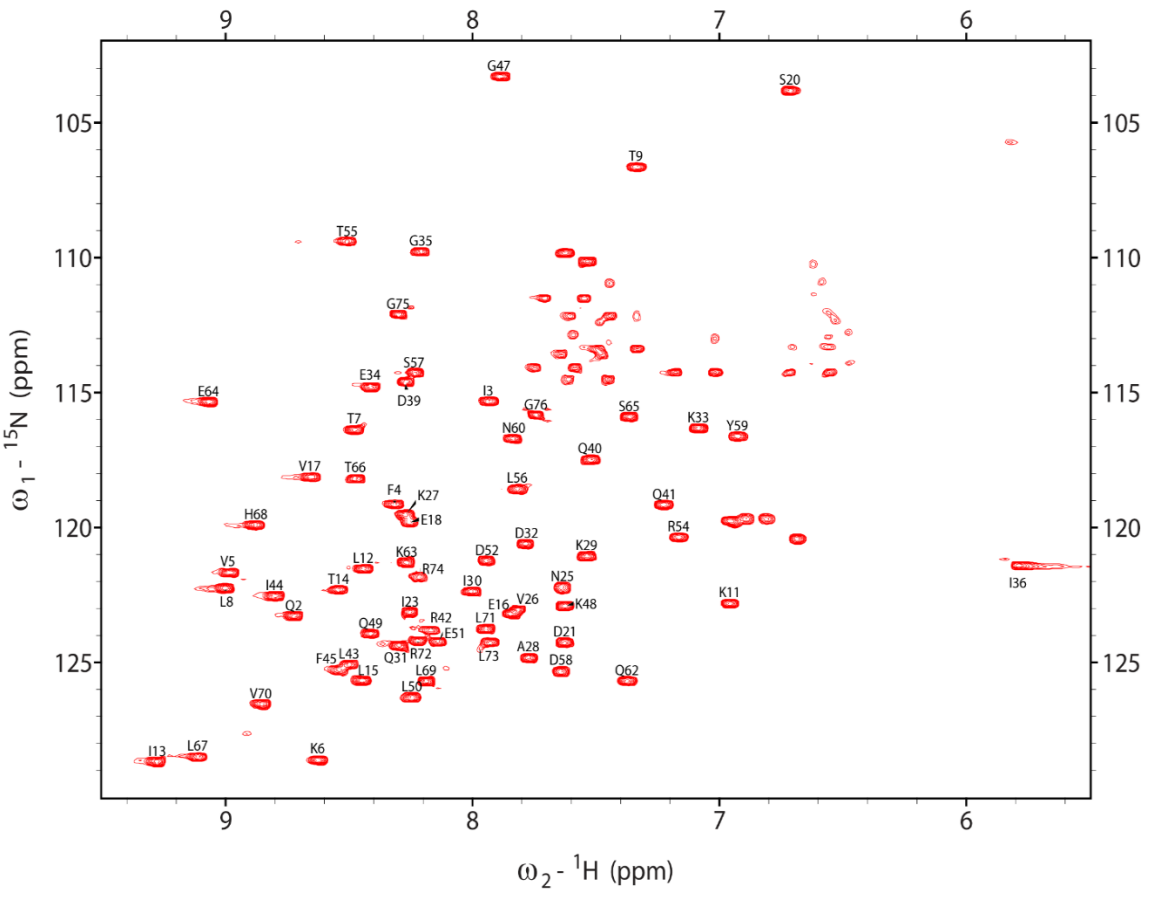

Reference ^{1}H-^{15}N HSQC spectrum of 500 µM ^{15}N ubiquitin at 5°C used for analysis.

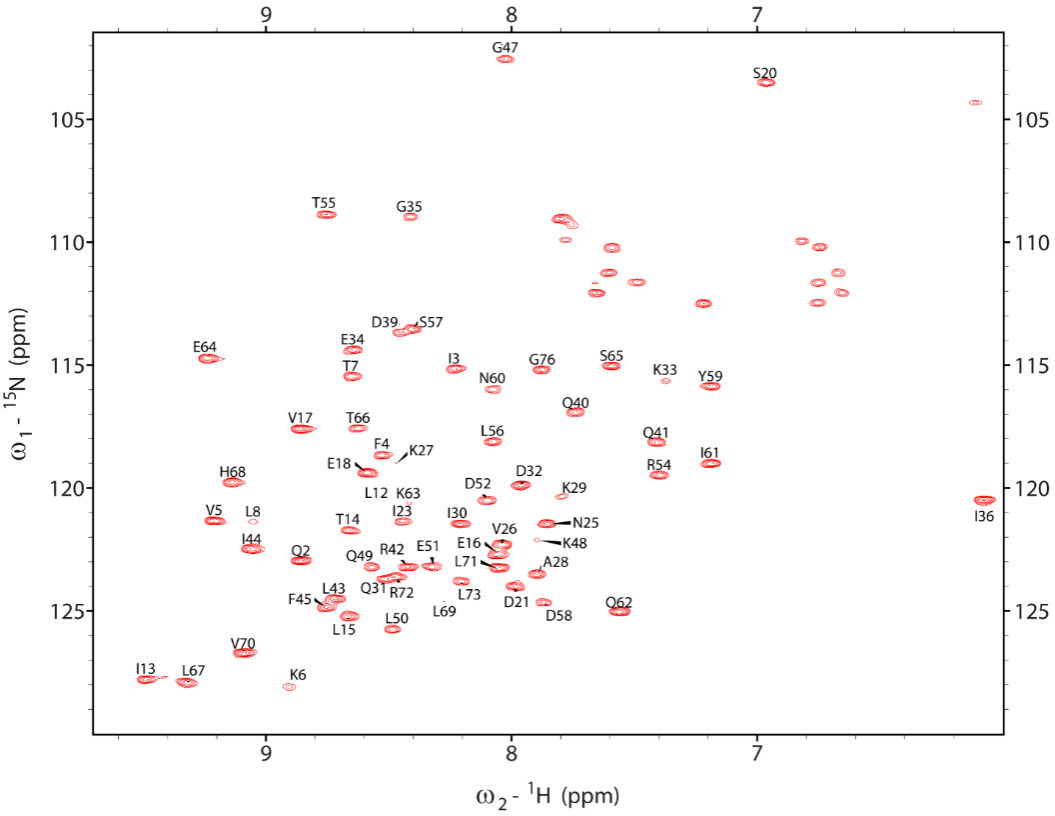

Reference ^{1}H-^{15}N HSQC spectrum of 500 µM ^{15}N ubiquitin at 25°C used for analysis.

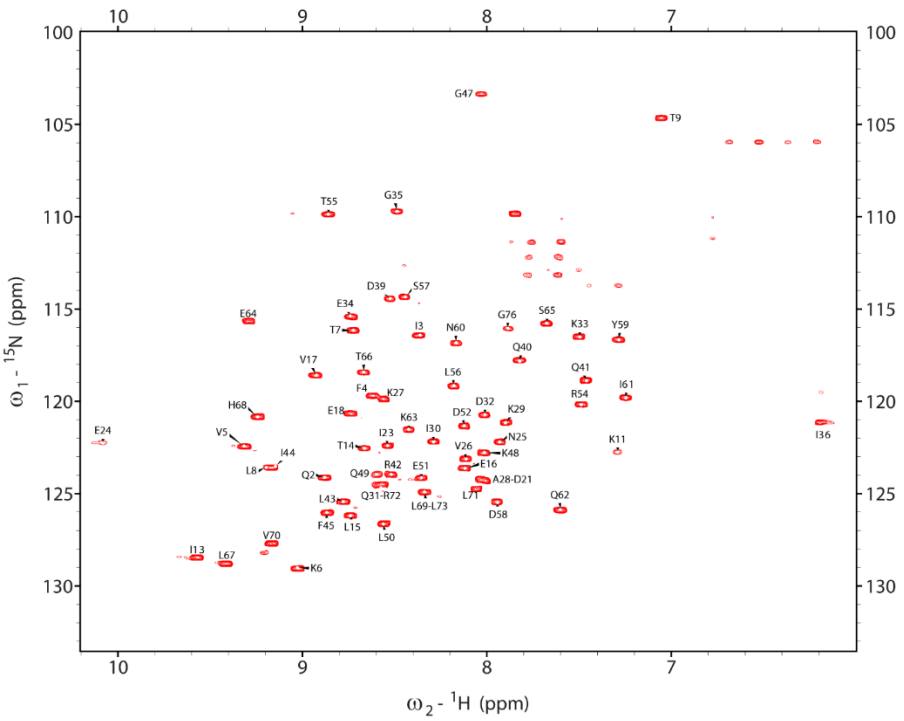

Reference ^{1}H-^{15}N HSQC spectrum of 500 µM ^{15}N ubiquitin at 45°C used for analysis.

4.3 Negative control spectra with polymer 2.

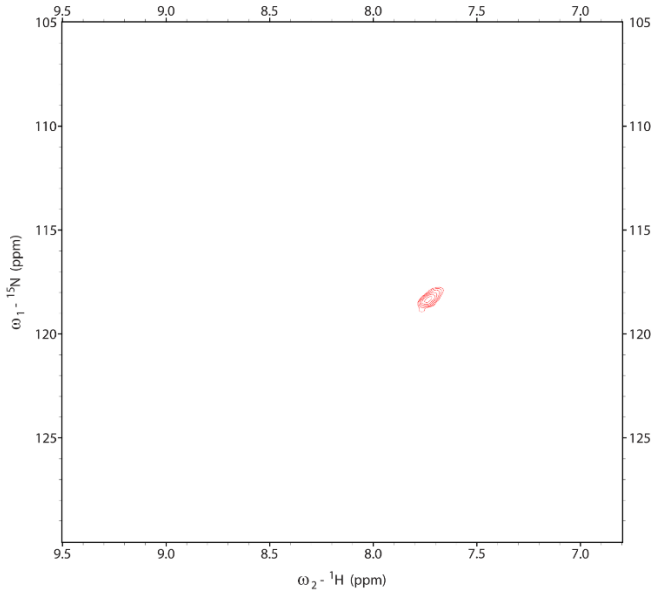

Reference ^{1}H-^{15}N HSQC spectrum of 10 mg/mL polymer 2 (EoEtA-mTrp) at 5°C used as a negative control.

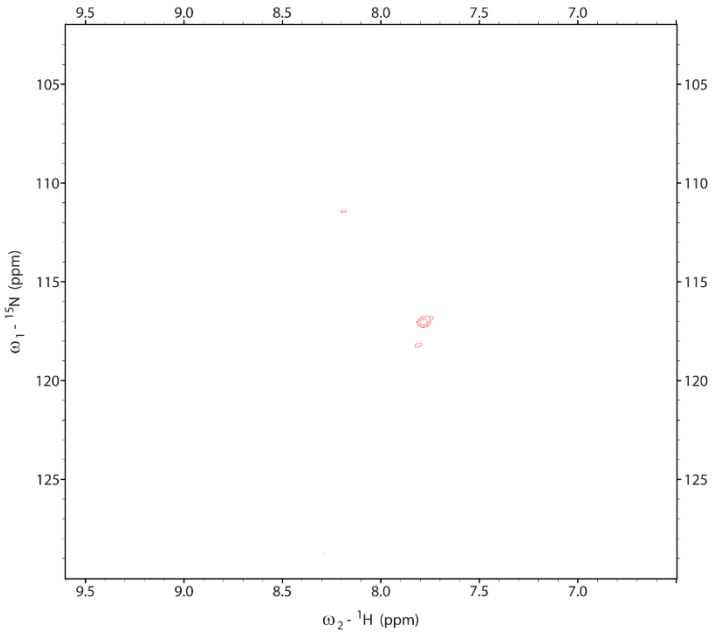

Reference ^{1}H-^{15}N HSQC spectrum of 10 mg/mL polymer 2 (EoEtA-mTrp) at 25°C used as a negative control.

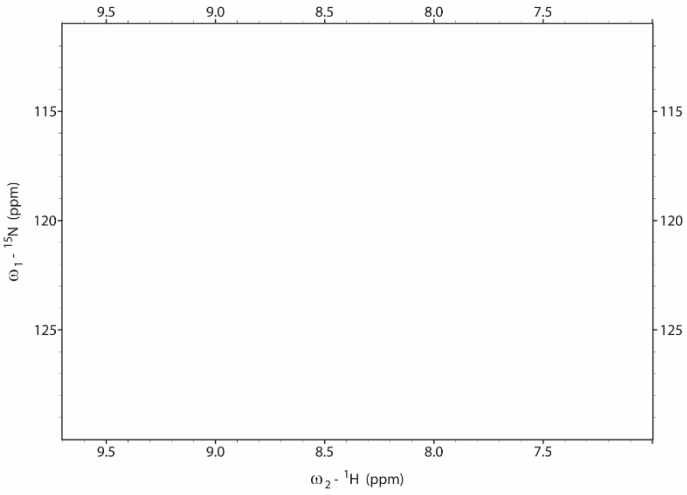

Reference ^{1}H-^{15}N HSQC spectrum of 10 mg/mL polymer 2 (EoEtA-mTrp) at 45°C used as a negative control. No observable signal within the contour level mimicking the other experiments.

APPENDIX FIVE

5.1 Experimental safety procedures

Standard safety precautions within a laboratory environment were taken while research was conducted. While conducting wet experiments and handling reagents, all skin below waist was covered, clothing was not loose fitting, personal ANSI z87.1 *fisherbrand* eyeglasses were worn, and gloves were worn. Sterile techniques were used when handling bacterial cultures and all samples to prevent contamination. A safety-buddy system was used when conducting French press cell lysis.